QATAR UNIVERSITY

COLLEGE OF HEALTH SCIENCES

THE CROSSTALK BETWEEN AUTOPHAGY AND INFLAMMATION DURING CO-INDUCTION WITH HYPERURICEMIA AND BACTERIA

BY

Nada Al-Emadi

Duha Al-Awad

A Project Submitted to the Faculty of College of health sciences in Partial Fulfillment of the Requirements for the Degree of Bachelor of Biomedical Sciences

Supervisors: Prof. Asmaa Al-Thani & Dr. Susu Zughaier

Abstract

Autophagy is a homeostatic process that regulates and recycles intracellular structures. In addition, autophagy a host defense mechanism that help reduce the burden of many infections. The inflammasome is a multiprotein structure that results in the release of proinflammatory cytokine after the preceding activation by danger signals. There is an apparent interplay between autophagy and the inflammasome to regulate inflammatory responses. Gouty arthritis is a commonly encountered inflammatory joint disease. The hallmark of this disease is hyperuricemia that results in the precipitation of monosodium urate crystals in the joints, leading to inflammation. A small subgroup of gout patients develops septic arthritis, which present a challenge during clinical diagnosis and is usually undetected. We aimed to investigate the effect of bacterial infection during hyperuricemia on autophagy and the inflammatory profile of macrophages. We hypothesized that during hyperuricemia the inflammatory response by macrophages will be aggravated. To test our hypothesis, we monitored the effect of bacterial infection during hyperuricemia on autophagy and on inflammasome activation in macrophages. To this end, we measured the following different cellular responses: autophagy flux, IL-1β release, and nitric oxide release. We found that uric acid enhanced autophagy and nitric oxide release, which resulted in an overall reduction in inflammatory response assessed as decreased IL-1β levels. These results suggest that uric acid exerts modulatory effects on autophagy and reduced inflammation during bacterial infection in macrophages. Uric acid in plasma acts as anti-oxidant and in certain conditions acts as inflammatory danger signal. Understanding the effect of uric acid on the interplay between autophagy and inflammation will facilitate therapeutic discovery and design.

الخلاصة:

عملية الالتهام الذاتي هي إحدى العوامل التي تساعد الخلية على المحافظة على بيئتها الداخلية عن طريق إعادة تدوير كيانات الخلية الداخلية غير الأساسية. كما أن عملية الالتهام الذاتي تعزز قدرة جهاز المناعة على مقاومة العدوى التي تسببها المتعضيات المجهرية عن طريق التهامها مما يؤدي إلى انحلالها. الجسيم الالتهابي يتكون من مجموعة البروتينات التي تعمل يدا بيد لإفراز عدد من السيتوكينات المسببة للالتهابات. تجتمع هذه البروتينات بعد استقبال الخلية للإشارات الدالة على وجود خطر على حياة الخلية. هناك رابط قوي بين عملية الالتهام الذاتي و الجسيمات الالتهابية. التهاب المفاصل النقرسي أحد أكثر التهابات المفاصل انتشارا. يتصف هذا المرض بوجود نسبة عالية من حمض البوليك في البلازما، مما يؤدي إلى ترسب كريستالات حمض البوليك في المفاصل و بالتالي يقع التهاب المفاضل. فئة قليلة من مرضى التهاب المفاصل النقرسي يعانون من التهابات بكتيرية مصاحبة للمرض، مما يصعب عملية التشخيص الصحيحة، و بالتالي يقلل من فرص وصف العلاج المناسب. في هذا البحث، هدفنا إلى دراسة تأثير الالتهاب البكتيري و فرط كمية حمض البوليك على عملية الالتهام الذاتي و تكون الجسيمات الالتهابية في خلايا الفأر البلعومية. لقد افترضنا ان فرط حمض البوليك سيؤدي إلى تفاقم الالتهاب البكتيري. لاختبار هذه الفرضية، قمنا بمتابعة ثلاث عوامل مختلفة لتعكس لنا تأثير الالتهاب البكتيري المصاحب لارتفاع حمض البوليك على عملية الالتهام الذاتي و تكون الجسيمات الالتهابية. هذه الثلاث عوامل هي: تدفق عملية الالتهام الذاتي، و افراز انترلوكين 1 بيتا، و كمية انتاج أكسيد النتريك. على عكس توقعاتنا، وجدنا ان فرط حمض البوليك عمل على زيادة عملية الالتهام الذاتي و كمية انتاج أكسيد النتريك، و لكنه تسبب في تقليل انترلوكين 1 بيتا خلال العدوى البكتيرية، و ترتب على ذلك انخفاض في حدة الالتهاب المصاحب للعدوى. من خلال النتائج المطروحة في هذا البحث، فإننا نقترح ان زيادة حمض البوليك تساعد على خفض حدة الالتهابات البكتيرية و الاعراض المترتبة عليها في مرضى التهاب المفاصل النقرسي.

Keywords:

Autophagy, inflammasome, uric acid, gout, NLRP3, nitric oxide

Table of Contents

List of figures

Acknowledgments

We would like to thank our supervisor Dr. Asmaa Al-Thani for providing the means to conduct this research, Dr. Nahla for providing bacterial strains, and Dr. Marwan Abu-Madi for providing additional reagents. We would like to extend our gratitude to Dr. Hanaa, Dr. Mahmoud, and Dr. Reham for helping us in the CMED laboratories. Mr. Alaa for helping us with confocal Imaging and Mr. Gelbin for running the flow cytometry. Last but not least, we are grateful for Dr. Susu Zughaier, our supervisor, who offered unconditional guidance, mentoring, and support and who went the extra mile in order for us to present this thesis.

The Crosstalk Between Autophagy and Inflammation During Co-Induction with Hyperuricemia and Bacteria

1. Introduction

1.1 Autophagy

Living cells are constantly degrading and synthesizing cellular components. The process in which an equilibrium of degradation and synthesis is maintained is termed 'autophagy'. Autophagy literally translates to self-eating, which is the process in which cellular homeostasis is maintained. Proteins and organelles are degraded through autophagy, providing basic materials for the synthesis of new cellular components. The hallmark of autophagy is capturing cytoplasmic compartments and bringing them to lysosomes for degradation (1). Loss of autophagy has been associated with many diseases such as cystic fibrosis (2), pulmonary hypertension (3), and inflammatory bowel disease (4), as well as other non-inflammatory chronic metabolic diseases.

1.2 Inflammation

Inflammation is a complex response of host machinery to initiate host defense and repair mechanisms. Although it is an important protective mechanism, the process of inflammation needs to be strictly regulated to avoid overactivated inflammatory response which leads to cellular damage and death. Interestingly, autophagy has been implicated in the regulation of inflammation by regulating the inflammasome (5). The inflammasome is a key player in inflammatory response. It is a multi-protein complex that activates the highly inflammatory cytokines of IL-1 family, IL-1β and IL-18 (6). Activation of the inflammasome occurs in response to sterile and non-sterile endogenous or exogenous agents. Autophagy reduces inflammation indirectly by eliminating danger associated molecular patterns (DAMPs), and pathogen associated molecular patterns (PAMPs). It also directly regulates the inflammasome by preventing the assembly of essential

inflammasome components (5). More interestingly, IL-1β which is the final product of inflammasome formation has a stimulatory effect on autophagy (7).

Another potent molecule associated with autophagy and inflammation is nitric oxide. Under normal physiological condition nitric oxide exhibits an anti-inflammatory effect on the body. However, impaired production of nitric oxide in certain diseases exerts a pro-inflammatory effect. Nitric oxide has been shown to have a paradoxical relationship with autophagy in which it induces and inhibits autophagy (8, 9).

1.3 Autophagy Inducing Agents

Autophagy is induced under starvation conditions and also can be induced by several agents including sterile inflammatory molecules such as soluble uric acid or bacterial pathogen associated molecular patterns (PAMPs) such as Lipopolysaccharides (LPS) (10). These molecules induce autophagy while at the same time influencing inflammatory mediators such as nitric oxide and IL-1β.

1.4 Objectives of the study

The role of autophagy in cellular regulation is revealing many mechanisms by which disease processes occur. However, the role of hyperuricemia in autophagy modulation has not been studied. Neither is the differences in autophagy modulation during sterile and non-sterile inflammation by hyperuricemia, Gram-positive, and Gram-negative bacteria respectively. In this study, we investigated whether there is a difference in autophagy modulation and inflammatory cytokine production under three different stimulation conditions hyperuricemia, whole cells formalin-fixed Gram-positive or Gram-negative bacteria, and co-induction with hyperuricemia and formalin-fixed bacteria.

2. Literature Review

2.1 The discovery of autophagy

The discovery of the lysosome set the foundation stone for the discovery of autophagy. The term 'lysosome' has been coined to the sac-like membrane containing hydrolytic enzymes more than 50 years ago (11). Shortly after the discovery of the lysosome, the mechanism through which cellular components are brought to lysosomes for degradation was recognized as 'autophagy' (12). It was soon recognized that autophagy occurs at basal levels in all cells, and in health and disease. Autophagy is induced in normal physiological processes such as cellular differentiation and aging. In addition, autophagy is stimulated by danger stimuli such as starvation states or by the presence of foreign material (13).

2.2 Types of autophagy

Up to date, three different forms of autophagy have been recognized. These are; microautophagy, chaperon-mediated-autophagy (CMA), and macroautophagy (14). Microautophagy is a form of autophagy in which component degradation occurs directly through lysosomal invagination (15). CMA is a unique form of autophagy. Instead of proteins being sequestered or engulfed, they are excluded from the cytosol and are translocated through the lysosomal membrane to the lumen where they are degraded by proteolytic enzymes (16). Macroautophagy (referred to as autophagy in this paper), the most prevalent and heavily studied form, occurs through sequestration of cytosol components into a double membrane known as the autophagosome. The lysosome then fuses with this double membrane and the sequestered compartments are digested (14).

Autophagy can be further classified to selective and non-selective autophagy. Non-

selective autophagy is the core degradation process and was once thought to be the only form of autophagy. It usually occurs in response to starvation and involves the sequestration of random parts of the cytosol which may or may not include organelles (17). Selective autophagy, as the name implies, describes the process in which specific cellular components are sequestered in the autophagosome and are then transported to the lysosome. Several forms of selective autophagy have been described, examples include; mitophagy (autophagy of mitochondria), pexophagy (autophagy of peroxisomes), reticulophagy (autophagy of endoplasmic reticulum) and xenophagy (autophagy of microbes) (18). The selections of compartments to for autophagy relies on autophagy receptors that are capable of recognizing their ligands on the various components (19).

2.3 Roles of autophagy

2.3.1 In cellular hemostasis

Now that the basic definitions regarding autophagy have been established, a concise description of the fundamental roles this process plays in health and disease is required. As mentioned earlier, autophagy maintains cellular hemostasis. It achieves this through regulation of what to be degraded and what to remain. Autophagy aids in the utilization of energy stores during starvation by contributing to the degradation of glycogen (20). A phenomenon which has been noticed in the early years of autophagy research, where glucagon was used as an autophagy inducer (13). Autophagy is also important in the maintenance of normal protein levels and organelle recycling. Mice studies provided highly suggestive evidence for the role of autophagy in cellular compartment turnover (21).

2.3.2 In disease

Deregulated or defective autophagy has been linked to many disease processes including myopathies, neurodegenerative diseases, cancers. In fact, the intense study of autophagy allowed

for the characterization of a new group of diseases known as autophagic vacuolar myopathies (AVM). The hallmark AVM disease is the accumulation of autophagy vacuoles in the muscle cells of affected patients. An example of AVM is Danon disease, a disease where patients suffer from cardiomyopathy, myopathy and mental retardation (22). Accumulation of autophagy vacuoles in mice was observed in the neural cells of mice deficit in autophagy. These mice showed signs of neurological dysfunction and ceased to live at an average age of 7 months (23). Huntington disease, a neurodegenerative disorder, has been associated with the impairment of autophagy. A consequence of a mutated Huntington protein (mHtt), which interferes with the action of Beclin-1 (BECN1), is its contribution to the protein homeostasis dysfunction observed in the disease (24). Autophagy has also been implicated in oncosuppression. Murine studies demonstrated that defective autophagy results in expedited oncogenesis (25). However, autophagy has also been shown to facilitate the growth of some cancerous cells by maintaining cellular hemostasis during starvation, introducing autophagy inhibition as a potential therapeutic solution for some tumors (26).

2.3.3 In immunity

The process of autophagy has also been shown to contribute to innate immunity. Autophagosomes containing intracellular have been shown to fuse with MHC-II loading compartments and result in improved antigen presentation to T cells (27). Moreover, autophagy plays a role in detecting and degrading invading microorganisms. Membrane damage is one of the danger signals that initiates autophagy of the damaged membrane and its content (28). Invading pathogens that damage their enclosing membranes (phagosome) within the cells provide targets for their destruction through autophagy (29). It is also worth to note that knock-down of Atg5 (autophagy related protein 5) in mice has shown decreased ability of immune cells to clear

intracellular infection, providing evidence for roles of the Atg proteins beyond autophagosome formation (30).

2.4 Canonical pathway of autophagy

Autophagy is induced by different stress factors, with starvation as the most commonly known stress factor. The presence of bacteria and recognition of dysfunctional organelles (e.g. mitochondria) can also trigger autophagy. The key steps of autophagy include an initiation signal provided by the unc-51-like kinase 1 (ULK1) complex. Autophagy proteins are then recruited at phagophore (isolation membrane) assembly site (PAS). Next, membrane nucleation occurs and phagophore forms. Ubiquitin-like conjugation systems then mediate the formation of autophagosome by elongation of the preexisting phagophore, lastly, the autophagosome is fused with the lysosome and its internal constituents are degraded and recycled (31).

2.4.1 Initiation

Inhibition of mTOR by starvation permits the activation ULK1 complex, which permits recruitment of autophagy proteins at the PAS. Omegasomes represent the PAS from which the phagophore arises and matures into an autophagosome. They generally originate from phosphatidylinositol 3-phosphate rich regions in the endoplasmic reticulum ER (32). The ULK1 complex is made through the association of ULK1 with Atg 13, FAK family kinase interacting protein of 200kDa (FIP200) and Atg101 (33, 34).

2.4.2 Membrane nucleation

ULK1 complex recruits the constituents of class III phosphatidylinositol 3 kinase (PI3K) complex, which are; phosphatidylinositol 3 kinase catalytic subunit 3 (PIK3C3), BECN1, PI3KR4/p150, Atg14L and nuclear receptor binding factor (NRBF2) (35-38). This PI3K complex

catalyzes the formation of phosphatidylinositol 3-phospate (PI3P), a membrane phospholipid that further recruits PI3P-binding autophagy proteins to the PAS, with WD-repeat domain phosphoinositide-interacting 2 (WIPI2) protein being the most significant (39-41). The significance of WIPI2 proteins arises due to the fact that this protein recruits Atg5-Atg12-Atg16 complex (41). In addition, Atg 9, the only transmembrane autophagy related protein, is speculated to contribute to phagophore biogenesis by bringing Golgi and endosomal membranes to the omegasome (42, 43).

2.4.3 Phagophore elongation

Phagophore elongation and its ultimate sealing leads to the formation of the autophagosome. This process is achieved by two ubiquitin-like conjugation systems, the Atg5-Atg12 and the Atg8/LC3-PE (Atg8 will be used for simplicity). Atg5-Atg12 is formed when the E1-like enzyme Atg7 brings Atg12 to the E2-like enzyme Atg 10. Atg5 then conjugates with Atg12 and Atg10 is released (44). Atg5-Atg12 the complexes with Atg16L1 and contributes to phagophore expansion (45). Atg8-LC3 forms when Atg7 brings Atg8 to the E2-like enzyme Atg3. This process is followed conjugation of Atg8 with phosphatidylethanolamine (PE) present on the growing phagophore (46). The Atg5-Atg12-Atg16 complex resembles E3-like enzyme which drives the conjugation of Atg8 to PE (46, 47)

2.4.4 Maturation and degradation

Once the autophagosome mature and encloses, it fuses with lysosomes for degradation of its content. RAB7A, SNAREs, PLEKHM1, and homotypic fusion vacuole protein sorting complex (HOPS) all function to degrade the autophagosome and its content (48-52).

2.5 Regulation of autophagy

Autophagy is regulated through the kinase mechanistic Target Of Rapamycin Complex 1 (mTORC1). This kinase is highly responsive to the nutritional status of the cell. In nutrient-rich conditions this kinase inhibits autophagy by phosphorylating the ULK1 complex preventing their participation in phagophore formation (53). Beside the inhibitory role of mTORC1, regulation of autophagy can be achieved by stimulatory signals. One of these signals is promoted by BECN1. As mention earlier, BECN1 is one of the constituents of the PI3K complex, which is responsible for the formation of PI3P during phagophore biogenesis. Since BECN1 function affects the summit of the autophagy hierarchy, regulation of this protein sets bases for regulation of autophagy as a whole. BECN1 is regulated by binding to proteins such as BECN2 or intermediate filament protein vimentin 1 (VMP1). Phosphorylation of BECN1 or its associated proteins releases BECN1 and allows it to participate in the formation of PI3K formation complex (19).

2.6 Autophagy induction during inflammation

Autophagy induction can occur via different pro-inflammatory molecules and receptors within cells. Those include receptors present in phagocytes, various pro-inflammatory cytokines and interleukins, as well as danger associated molecular patterns (DAMPs).

Autophagy is induced by various receptors present in phagocytes such as toll-like receptors (TLR), nucleotide binding oligomerization domain (NOD)- like receptors (NLR), as well as retinoic acid-inducible gene (RIG-1)-I-like receptors (RLRs). Stimulation of TLRs can induce autophagy which provides an antimicrobial response (54). On the other hand, autophagy can also induce TLRs by the transport of microbe derived pathogen associated molecular patterns (PAMPs) to the endosomal lumen which activates TLR (55). Likewise, NOD1 and NOD2 which are NLRs

have shown to recruit ATG16L at the site of bacterial entry in the plasma membrane (56). To add, NLRX1 promotes the formation of autophagy related complexes ATG5-ATG12-ATG16L (57). The RLRs stimulation is augmented by Atg5 deficiency through increased levels of reactive oxygen species (ROS).

Several types of cytokines are involved in the promotion of autophagy such as TGFβ, IFNγ, TNFα, IL-2, IL-1α, and IL-1β. Tumor growth factor β (TGFβ) is implicated in the promotion of autophagy in multiple studies. The first study to describe the relationship treated bovine mammary epithelial cells with TGF-β1, which led to a significant increase in the levels of LC3 and Beclin-1 in their cytoplasm (58). Since then, many other studies showed that TGF-β promotes autophagy. It was found to induce autophagy in renal proximal tubular epithelial cells of human origin, human lung fibroblasts, breast cancer tumor stromal cells, and in human atrial myofibroblasts (59-62). Moreover, Interferon gamma (IFNγ) has been shown to induce autophagy formation in *Mycobacterium tuberculosis* infected macrophages (63). Likewise, Tumor necrosis factor-alpha (TNF-α) has shown comparable results. When JEG-3 cells are treated with TNF-α showed a significant increase in the expression of LC3-II which indicates increased autophagy (64). Another potent cytokine in the induction of autophagy is IL-2, which promotes autophagy in natural killer cells and lymphocytes rather than macrophages (65). When cancer patients are treated with IL-2 they experience systemic autophagy, which sometimes lead to systemic autophagic syndrome that results in organ dysfunction (65). Furthermore, IL-1α and IL-1β enhance autophagy by activating autophagosome formation (66, 67). Interestingly, these interleukins are also inhibited by autophagy, which could propose a negative feedback mechanism.

Danger associated molecular patterns (DAMPs) are known inducers of autophagy. These molecules include HMGB1, DNA, and S100A8/A9 are released by cells under various conditions

of tissue damage. One well studied DAMP is the chromatin regulating high mobility group box 1 (HMGB1) protein, which is found abundantly in the nucleus (68). Increased levels of reactive oxygen species promote HMGB1 to translocate to the cytoplasm where it interacts with Beclin1 protein to promote autophagy (68). Furthermore, when DNA is leaked out of the nucleus and mitochondria autophagy can be induced via poly-ADP ribose polymerase-1 (PARP-1) (69). To add, S100A8/A9 complex is a complex of the S100 Ca^{2+} protein binding family that are found in different cell types and are expressed abundantly in myeloid cells (70). When SHEP cells are treated with S100A8/A9 typical autophagy structural hallmarks under electron microscopy, as well as increase in Beclin-1 expression in addition to Atg12-Atg5 formation in those cells (71). These findings indicated a role of autophagy in S100A8/A9 induced cell death (71).

2.7 Inflammation

The term inflammasome was first described in 2002 by Tschopp *et al.* to describe a high molecular weight structure containing multiple-inflammatory proteins (72). This structure orchestrates the activation of caspase-1 which leads to the formation of pro-inflammatory cytokines IL-1β and IL-18. Since then, research has expanded in this area and different inflammasomes have been described. The initiation of inflammasome formation is done by various cytosolic sensor proteins. These sensors are proteins which include NOD like receptor members (NLR) NLRP1, NLRP3, NLRC4, in addition to AIM2, and pyrin.

2.7.1 NLRP3 inflammasome

The most widely studied inflammasome is NLRP3 (73). The inflammasome structure is simple and consists of NLRP3 protein, adaptor ASC protein, and pro-caspase-1 (74). The activation of NLRP3 inflammasome requires two signals a priming signal, which upregulate the formation of NLRP3, pro-IL-1β, and IL-18m and a secondary signal which triggers the assembly

of the inflammasome complex (75). NLRP3 protein has three domains which are leucine rich repeat (LRR), NACHT region, and pyrine domain (PYD).

NLRP3 senses danger signals via its LRR region at its C-terminal which leads to its activation. Then, it undergoes oligomerization by interacting with the pyrin domain of adaptor speck like protein containing C-terminal caspase recruitment domain (ASC) (72). ASC activates procaspase-1 to its active form by proteolytic cleavage through cysteine protease pro-caspase-1. Caspase-1 proteolytically activates IL-1B and IL-18. It also has a role in the initiation of pyroptosis which is a form of inflammatory cell death (76). NLRP3 can be activated by several molecules such as PAMPS, DAMPS, crystalline influx, and ATP influx (77).

2.7.2 NLRP1 inflammasome

This is the first NLR to be described in the formation of inflammasomes (72). This pathway of inflammasome formation is activated by various signals such as *Bacillus anthracis* lethal factor, muramyl dipeptide, *Toxoplasma gondii*, as well as intracellular ATP depletion (78).

2.7.3 NAIP-NLRC inflammasome

This inflammasome has been shown to be activated by bacterial flagella and type three secretion system (T3SS) which delivers bacterial virulence factors to block host defense. NAIPs binds to bacterial flagella and T3SS, then interact with NLRC4 which acts as an adaptor protein to enable the activation of caspase-1 (79).

2.7.4 AIM2 inflammasome

Absent in melanoma 2 protein (AIM2) is a protein that recognizes double-stranded DNA within cellular cytosol (80). It can be initiated by double stranded DNA from various pathogens such as bacteria and viruses. However, it can also be initiated by host DNA in the cytosol. Thus,

any condition leading to the accumulation of host DNA in the cytosol would lead to activation of inflammatory responses (80).

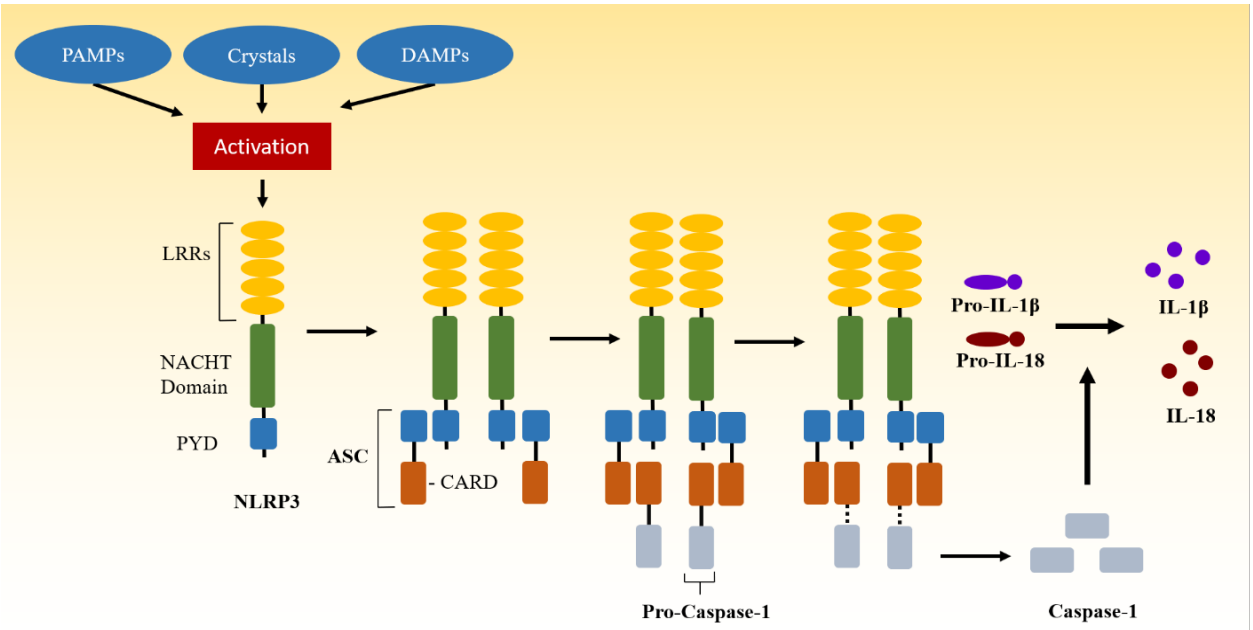

Figure 2-1 Activation of NLRP3 inflammasome

Different molecules such as PAMPs, DAMPs, as well as crystals such as MSU crystals can activate the NLRP3 inflammasome. Oligomerization occurs between ASC and NLRP3. Pro-caspase-1 is activated by ASC and is proteolytically cleaved to caspase-1. Caspase converts pro-IL-1β and pro-IL18 to IL-1β and IL-18 which exist the cell to perform various functions.

2.7.5 Pyrin inflammasome

The pyrin inflammasome is activated via sensing various bacterial toxins (81). *MEFV* gene is the gene coding for pyrin protein and mutations in this gene are linked to hereditary autoimmune diseases (82).

2.8 Nitric Oxide

2.8.1 Nitric Oxide Synthesis and Function:

Nitric oxide is a free radical considered as a reactive nitrogen species that acts as a signaling molecule. It is an abundant cellular messenger found throughout the body, in the

nervous, cardiovascular and immune systems. It has a multitude of functions in which is elicit physiological responses such as regulating blood flow and tissue response to hypoxia, as well as autophagy (83). It is synthesized by nitric oxide synthases from the amino acid L-arginine in a two steps oxidation process (84).

2.8.2 Nitric Oxide and the Inflammasome:

Nitric oxide is known to be a strong inhibitor of cytokine expression (85). It has been found to inhibit the activity of caspase-1 enzyme. This ultimately leads to the inhibition of the inflammasome, and the release of IL-1β and IL-18 even in the presence of (86). Even when RAW 264.7 macrophages were induced with LPS, the presence of nitric oxide still led to the inhibition of IL-1β production (87).

2.8.3 Nitric Oxide and Autophagy:

The interplay between nitric oxide and autophagy is a complex process (88). This is due to the paradoxical relationship between nitric oxide and autophagy, in which the literature shows both inhibitory and stimulatory effect of nitric oxide on autophagy (9, 89). Under the conditions of sever oxidative stress nitric oxide was found to promote autophagy (90). Another study found that overexpression of nitric oxide actually impairs autophagy machinery by decreasing JNK1 and Bcl-2 phosphorylation and activation mTORC1 (9). On the other hand, Pestana *et al.* found that inhibiting autophagy stimulated nitric oxide levels in human umbilical vascular endothelial cells (91). The contradictory effect of nitric oxide on autophagy suggest the presence of a feedback loop between autophagy and nitric oxide that remains to be elucidated.

2.9 Uric acid as an inducer of inflammasome formation

Purine catabolism leads to the production of uric acid, which is a danger associated molecular pattern that is released from dying cells and ischemic tissue (92). When uric acid crystalizes, it activates the immune system.

Accumulation of uric acid in the body occurs due to increased production with unavailability of a degradation enzyme. Humans lack uricase enzyme that has the ability to convert uric acid to a more soluble product, allantoin (93). It is thought that loss of this enzyme by silencing the gene responsible for its production is an evolutionary process that provided a survival (94). Although uric acid crystals have antioxidant properties when present in body fluids at normal physiological levels (95). In contrast, t higher concentrations it appears to act in a reversible pro-inflammatory manner. This is implicated in the uptake of uric acid by adipocytes, which leads to the activation of NAPDH oxidases (96).

When a cell is dying or is ischemic it releases danger signals to alert the body defenses and to promote tissue repair (97). One of these molecules is uric acid which is released from the cells in the soluble form. However, after exceeding 6.8 mg/dL concentration in a solution, uric acid crystals begin forming with the aid of other enhancing factors such as low temperatures and acidic environments (98-100). Uric acid crystals are detected by phagocytes such as monocytes and macrophages. Once phagocytes engulf uric acid crystals, a cascade of signaling within these cells is initiated to promote inflammation. However, it is not clear how these crystals interact with phagocytes to trigger phagocytosis and signaling within cells (101).

Some studies suggest that uric acid crystals are recognized by the immune system, and

antibodies against the crystals form and coat them. Then, antibody coated crystals are recognized by antigen presenting cells through interacting with the Fc portion of the antibody (102). Also, Monosodium urate crystals that are coated with IgG antibodies promote the production of reactive oxygen species in phagocytes after engulfment (103). Another mechanism shown by Naccache *et al.* is the direct binding of monosodium urate crystals with CD16 receptor also termed as FcγRIII receptor on the surface of neutrophils (104).

Recently, uric acid has be classified as a danger molecule (105). Uric acid crystals have (106). The mechanisms by which uric acid crystals activate inflammasome formation are discussed below. Uric acid causes potassium efflux which is a known initiating signal that triggers the activation of NLRP3 inflammasome (107). Also, crystals are too large to be phagocytosed, which leads to a process called frustrated phagocytosis (108). Ultrastructure studies have shown that uric acid crystals, despite their size, can still be phagocytosed by phagocytes. However, the phagolyososomes that form have disrupted membranes and could possibly release part of their content into the cytoplasm (109). Damaged lysosomes release cathepsin B which mediates inflammation (110). To add, uric acid crystals also produce ROS which also activates inflammasomes (96).

Until recently, it was thought that uric acid in the soluble form is inert and doesn't initiate an inflammatory response. However, Braga *et al.* have shown that soluble uric acid can activate the NLRP3 inflammasome through the production of mitochondrial reactive oxygen species (111).

Indeed, soluble uric acid has an inflammatory effect, but the causative agent of gout remains to be the uric acid crystals that forms due to hyperuricemia in addition to enhancing factors. It is highly inflammatory and leads to the formation of inflammasomes, release of IL-1β

which leads to the rapid activation of neutrophils. These molecular mechanisms lead to the disease known as gouty arthritis. Hyperuricemia, its implications, and gout disease will be discussed in the next section.

2.10 Hyperuricemia and gout disease

The most common cause of inflammatory arthritis is gout (112). The disease affects around 8.3 million people in the US (113). It was widely known that uric acid is elevated in the blood of patients with gout. However, it was only confirmed to be the causative agent of gout after proving that intra-articular injection of sodium urate crystals leads to the development of gout.

Gout occurs due to the presence of constantly elevated levels of uric acid in the blood which eventually lead to the deposition of crystals in joints. Although the condition is treatable, it is extremely painful. Hyperuricemia and gout have common risk factors namely age, alcohol consumption, renal impairment, diuretic therapy, male gender, postmenopausal women, and genetic factors (114).

Concentration of uric acid greater than 6.8 mg/dL could lead to the formation of uric acid crystals that accumulate in joints (98). The development of gout disease varies from one person to another. However, there are three main steps of the disease formation (115). The first step includes hyperuricemia that is asymptomatic. Although hyperuricemia is implicated in gout development, many individuals experience hyperuricemia without developing gout. If the person is to develop gout, then he/she will suffer from the second stage. This stage includes periodic attacks of acute gout followed by remission and asymptomatic period. During this stage, when symptoms appear, they will be in form of fever, chills, and sever pain in the joints. At the final stage, the persistence of the second stage would lead to the development of chronic gout. The attacks in the chronic stage

are less painful, however the damage in the joints causes them to be chronically stiff and swollen (115).

Hyperuricemia is not only associated with gout, it is also associated with other disease conditions. It is observed in women with pre-eclampsia and is associated with the severity of the disease (116). A recent study suggest that hyperuricemia could serve as a predictive marker for the progression of nephrosclerosis (117). Another study observing breast cancer patients concluded that high uric acid levels in the blood indicates poor survival rate in those patients (118). Furthermore, hyperuricemia was described in various other conditions such as atherosclerosis, hypertension, cardiovascular diseases, as well as chronic kidney diseases (119).

Taken together, elevated levels of uric acid in the body is linked to various diseases ranging from kidney failure to hypertension. However, uric acid crystals are well known for being the causative agent of the disease gout. The disease progresses through several stages until it leads to chronic inflammation of the joints. The mechanism by which uric acid crystals cause inflammation is described in the previous sections.

2.11 Autophagy and the Inflammasome

As can be seen from the previous sections, autophagy and inflammasomes have key role in inflammation and response to cellular perturbations or death. They share common promotors in which they are both stimulated by a wide range of pro-inflammatory molecules such as DNA, DAMPs, interleukins, and cytokines. Not only that, but also autophagy have been shown to have regulatory effect on inflammasomes.

The role of autophagy in inflammasome regulation was first proposed in a study showing that ATG16L1 deficient mice had higher levels expression of IL-1β than wild-type mice. To add,

when those mice were also exposed to MSU or ATP which activate NLRP3, even more IL-1β production was observed (120). In another study, macrophages from LC3 deficient mice and mice lacking one normal allele of Beclin-1 experienced increased secretion of IL-1β and IL-18 in comparison to macrophages from wild type mice (121). As discussed earlier, IL-1β and IL-18 are produced because of inflammasome activation. Thus, the increase of these products in the presence of deficiency in autophagy implies that autophagy could have an inhibitory role to inflammasome activities.

The mechanism by which autophagy regulates inflammasomes is not yet fully understood. However, different mechanisms have been proposed in which autophagy either sequester inflammasome activators or proteins required for inflammasome functioning. Autophagy can possibly inhibit inflammasomes is by the removal of damaged mitochondria which automatically leads to the reduction of mitochondrial derived DAMPs release (121). This leads to the suppression of the inflammasome perhaps by the reduction of ROS which are responsible for NLRP3 inflammasome formation (122). Another way by which autophagy can inhibit inflammasomes is by p-62 dependent degradation of inflammasomes. When the NLRP3 and AIM2 inflammasomes are stimulated, K63-linked polyubiquitination of ASC is triggered. This is then recognized by the ubiquitin sensor p-62 which leads to targeting ASC to autophagosome for its degradation (123). Another study showed that in-fact autophagy can sequester pro-IL-1β into autophagosomes for its degradation when macrophages are treated with rapamycin, which is an inducer of autophagy (7).

2.12 Autophagy Induction During Microbial Infection

In the past, autophagy was thought to be a non-selective process meant for the bulk degradation of proteins. However, it was found that autophagy can also selectively remove unwanted proteins from cells by ubiquitylating them. This leads to a cascade of interactions with

various proteins that eventually degrades these components (124). A form of selective autophagy that is present within the cells is xenophagy. It is involved in the degradation of intracellular pathogens, and is considered to be a part of the innate immune response (125). The vacuoles that form when intracellular bacteria are engulfed are similar to autophagosomes. Both structures have LC3 molecules and their formation requires Atg5, which are proteins essential for autophagy (126). However, they differ considerably in size in which autophagosome diameter is between 0.5-1.0 μm while the Group A streptococcus (GAS)-containing autophagosome like vacuoles (GcAV) measure around 10 μm (127).

There are four proposed pathways for bacteria targeted autophagy Fusion of bacteria-containing phagosomes with lysosomes, autophagosomal membrane envelopment of bacteria-containing phagosomes or endosomes, the fusion of an autophagosome with a bacteria-containing phagosome or endosome, and the capture of bacteria that has escaped inside the cytoplasm by xenophagy. In some instances, the route of which the bacteria is lysed by autophagy is well-known such as group A streptococcus which escapes from endosomes and is captured in the cytoplasm (127). However, for other types of bacteria the mechanisms are not yet well known. Moreover, the general cellular mechanism used to target bacteria into phagosomes is thought to be similar to selective autophagy. The bacteria is tagged by cellular markers such as ubiquitin which interacts with adaptor proteins like p62 and NBR1. Those adaptor proteins have LC3 containing regions which acts as a target for autophagy (124).

The proteins involved in the process of xenophagy are important in protecting the host from infections. For example, a knockout of Atg5 in macrophages and neutrophils of mice increases their susceptibility to infection by *Listeria monocytogenes* and *Toxoplasma gondii*.

2.13 Microbial pathogens fight back

Microorganisms have developed certain measures to evade host response, and ultimately adapt to, escape or even hijack the autophagy mechanism. Below, different mechanisms of autophagy evasion are discussed.

2.13.1 Inhibiting autophagy initial signals

Some bacteria escape autophagy by avoiding the formation of the phagophore and inhibiting the initial signals leading to autophagy. Examples of such bacteria are *Salmonella typhimurium* and *Mycobacterium tuberculosis. S. typhimurium* initially does not escape autophagy, however at four hours post infection, the bacterium initiates an escape mechanism by promoting mTORC1 activation (128). The activation of mTORC1 leads to its relocation from the cytosol to the endosomes and vesicles containing *Salmonella* which inhibits autophagy targeted against it (128).

Moreover, *Mycobacterium tuberculosis* escapes autophagy by blocking a required trigger for autophagy initiation which is reactive oxygen species (ROS). This is done by the Eis gene which encodes for an N-acetyltransferase that activates a JUN N-terminal kinase (JNK)-specific phosphatase thus leading to its inactivation. When JNK is inactivated, the production of reactive oxygen species is blocked (ROS) thus, autophagy is not triggered (129, 130).

2.13.2 Direct interference with autophagy components activity

Shigella flexneri produces an effector protein VirA which inactivates RAB1 which is a GTPase mediating the trafficking from endoplasmic reticulum to the Golgi Apparatus (131, 132). Similarly, *Legionella pneumophila* produces an effector molecules RavZ which deconjugates PE from LC3 permanently leading to the inhibition of autophagosome formation (133).

2.13.3 Camouflage to avoid autophagy

In addition to directly interfering with autophagic components activity, *Shigella flexneri* can also avoid autophagy completely by masking itself. This is done by the action of IcsB which is secreted by type III secretion system. IcsB binds to IcsA present on the bacterial surface and act as a competitor to ATG5 binding, thus it masks the bacteria from recognition by the host machinery (134). To add, the lack of IcsB in mutant strains leads to the formation of cage like structures that heavily surround the bacteria. These structures are formed by septins which are important proteins for the recruitment of autophagy-initiating proteins (135).These findings suggest that IcsB can mask septins from recognizing bacterial cells, thus preventing the initiation of autophagy.

2.13.4 Blocking the fusion of autophagosome and lysosome

Some bacteria accumulate in autophagosomes however, these vesicles remain non-acidic and non-degradative during the period of infection. Thus, indicating the bacteria inhibiting the fusion of autophagosomes with lysosomes. Although it is known that certain bacteria exhibit such mechanism, it is yet to be known how the blocking of fusion is done. *Mycobacterium marinum* is one example of bacteria being sequestered into LC3 positive phagosomes that are positive for RAB7 and LAMP1 proteins yet, they do not acquire lysosomal activity and are non-degradative (136). Adherant-invasive *Escherichia coli* also known as AIEC shows a similar pattern, in which the bacterial cells are trapped within autophagosomes that never mature to into degradative autolysosomes which enables bacterial survival within these vesicles (137).

2.13.5 Hijacking Autophagy Machinery

Some bacteria do not stop at the inhibition of the killing functionality of autophagy. They exploit autophagy to promote their own growth and development. More interestingly, those bacteria can show lack of survival in cells that are not capable of performing autophagy. Majority

of the time, these bacteria work by inducing autophagy yet, blocking it at the stage of autophagosome thus, inhibiting the formation of autolysosome. Then, the bacteria is able to use this vesicle as a habitat for their growth and replication.

A well-known example undergoing this mechanism is *Staphylococcus aureus* which gets isolated into a double membraned autophagosome upon infection. However, the fusion of the autophagosome with lysosomes is inhibited and the bacteria survives and replicates within the autophagosome (138). After bacterial replication, the bacteria escapes into the cytosol and leads to cell death by autophagy which is dependent on the hosts' ATG5 (138).

Another example is the causative agent of Q-fever *Coxiella burnetii*. The bacterium is able to survive in host cells after infection within large replicative vacuoles, while producing proteins that inhibit cellular apoptosis to ensure their continuous growth and replication (139, 140).

2.13.6 Other escape mechanisms

Some bacteria that are known to be targeted by autophagy can escape the process using mechanisms that are yet to be known. These bacteria use their effector proteins and virulence factors to alter/avoid the normal autophagy process, however the targets of these proteins and how they work are not yet established. An example for such bacteria is *Burkholderia psuedomallei* which uses its type III secretion system to escape the phagosome into the cytosol and continue its replication cycle (141).

After setting the foundations of autophagy and its relation to cellular homeostasis, immunity, and inflammation, it is safe to address the purpose of this study. In this study, we compare the effect of sterile inflammation versus bacterial infection on autophagy. Provided the literature review, we speculate that during sterile inflammation and bacterial infection the

autophagy will be stimulated. However, we will monitor the extent of stimulation of autophagy and cytokine production and the inflammatory response during both process and grasp a better understating of the difference governing these processes. We also aim to examine the ability of macrophage to eliminate uric acid crystals after autophagic induction, a phenomenon which has not been examined yet.

3. Materials and Methods

3.1 Reagents

Uric acid sodium salt, DMSO, Bovine Serum Albumin (BSA), Paraformaldehyde, Orthophosporic acid and Sulfuric acid were purchased from Sigma Chemicals (Sigma USA). Dulbecco's modified Eagle medium (D-MEM), Fetal Bovine Serum (FBS), Penicillin/Streptomycin solution, 0.4% Trypan Blue were obtained from Gibco via Thermo Fisher scientific (USA). Mouse IL-1β ELISA DuoSet kit from R&D systems (Minneapolis, MN). Autophagy Detection kit was obtained from abcam (Cambridge, UK). Nutrient agar, Petri dishes, peptone, yeast extract, LB broth, and Phosphate Buffered Saline (Dulbecco A) tablets were obtained from Oxoid via Thermo Fisher (USA). Sulfonamide, N-(1-Naphthylethylenediamine) dihydride, and Sodium nitrite ($NaNO_2$) were purchased from Biochem Chemopharma (FRANCE). DAPI dilactate and propidium iodide obtained from Invitrogen (USA). Liquicolor uric acid detection kit was obtained from EKF Diagnostics (USA).

3.2 Cell cultures

Murine macrophages cell line RAW 264.7 was obtained from ATCC and GFP-LC3-stably transfected RAW264.7 cell line was a kind gift from Dr. Alfred Merrill, Georgia Institute of Technology, Atlanta, GA. Frozen stocks of macrophages were maintained in liquid nitrogen for long term storage. Macrophages were propagated in DMEM media supplemented with 10% (v/v) FBS, 50 IU/mL of penicillin, and 50 µg/mL of streptomycin and incubated in 5% CO_2 at 37^{o}C for at least 3 days. Once cells exhibited a confluency of approximately 80% new culture stocks were prepared. Cells were scraped manually and 5% DMSO was added to the cells. One mL of early passages of cells was transferred into labeled cryo-vials which then frozen and

stored in liquid nitrogen for long term storage. Several vials of RAW 264.7 and GFP-LC3-RAW were stored at -80ºC for short term storage and immediate use.

3.3 Cell Cultures propagation and maintenance

GFP-LC3-RAW264 and RAW264.7 were propagated into T75 cell culture flasks containing 25 mL culture media and incubated at 37ºC with 5% CO_2 under humid conditions. Cells were propagated once they exhibited overgrowth. Old cultures (older than a week) were discarded and a new set of RAW264.7 and GFP-LC3-RAW cells were revived from cell culture stock stored at -80ºC to replace old cultures as necessary.

3.4 Bacterial Culture & Fixation

Five different strains of clinically important Gram positive and Gram negative bacteria were kindly provided by Dr. Nahla Eltai and Dr. Asmaa Al-Thani at Biomedical Research Center of Qatar University. The following Gram positive bacterial strains were used in the experiments: *Staphylococcus aureus* (*S. aureus*) that is sensitive to antibiotics; low level Methicillin resistant *S. aureus* (MRSA-LR) and high level resistance *S. aureus* MRSA-HR. In addition to two Gram negative strains a sensitive *Klebsiella pneumoniae* strain and another *K. pneumoniae* strain resistant to β lactam antibiotics. Bacteria were cultured on nutrient agar prepared in the laboratory as follow: 500 mL of nutrient agar was prepared by mixing 2.5g peptone, 1.5g yeast extract, 7.5g agar, and then dissolved in 500mL of deionized water. The media suspension was autoclaved at 121ºC and 15 psi for an hour. The media was left to cool at around 60ºC and 25 mL was pipetted into sterile petri dishes. The dishes were left to solidify and cool down overnight and were flipped the next day. Freshly grown bacteria were harvested and immediately fixed in 10 mL of formalin solution to inactivate bacteria without lysis. Formalin solution (10% v/v) was prepared by diluting 40% formaldehyde in sterile PBS at 1:10 ratio. Bacterial isolates

were cultured and incubated at 37ºC for 24 hours, then harvested and resuspended in 10mL of 10% formalin solution, vortexed, and placed on rotator overnight at room temperature. To collect the fixed bacteria, the tubes were centrifuged at 5500 rpm for 15 minutes and were washed twice with sterile PBS to remove any traces of formalin. Pelleted bacterial cells were resuspended in 3 mL PBS. Bacterial density was assessed by measuring the optical density (OD) of the suspension at 600 nm wavelength in 1 mL cuvette using the spectrophotometer. The measured OD was then adjusted to 3 for each type of bacteria.

3.5 Uric Acid Preparation

50 mg of Uric acid dry crystals powder (UA) was added to 50 mL culture media and heated at 200 °C for 1 hour. A sterile syringe and a 45nm Sartorius syringe filter were used to remove large crystals. The final uric acid concentration was measured using Liquicolor uric acid quantitation kit following the manufacturer instructions with a modification to the blank. 20 microliters of media without uric acid is added to the blank to account for the color or remnants of uric acid present in the supplemented media. The initial measurement concentrations were above the recommended maximum values (20mg/dL) that maintain linearity of measurement. Therefore, dilutions of the concentrated sample were made and their concentrations were measured. Dilution with acceptable readout were used to determine the original uric acid concentration in the sample. The measured uric acid concentration was approximately 38 mg/dL.

3.6 Macrophage Induction Assay

Freshly grown macrophages (RAW264 cells and GFP-LC3-RAW264) were harvested by scraping the surface of the culture flasks and each cell line was pooled together in one main suspension to assess viability, cell density and adjust cell counts to similar density through all experiments.

3.7 Cell Count

An aliquot of 100 µL of media of the harvested cells was added to an Eppendorf tube containing 100 µL of 0.4% Trypan blue stain. Cell suspension was mixed well by tapping and pipetting up and down then 10 µL of the mixture was added to one chamber of a Luna hemocytometer. Hemocytometer was inserted into Luna II Automated Cell Counter to record cell count and viability. Viability above 85% was considered suitable for experiments.

3.7.1 Macrophage preparation and induction in 6-well plate

Based on the number of living cells obtained from the cell counter, cells were adjusted to half a million cells/mL. Coverslips were disinfected by dipping them in media containing penicillin/streptomycin, and one coverslip was added into each well. Two mL GPLC3-RAW264 containing media were seeded into two 6-well plates with final density of 1 million cells per well. Cells were allowed to settle in the incubator for 30 minutes. Adherence was confirmed by visualizing cells under the microscope. Next, one of the two 6-well plates was labelled as 'Uric Acid', indicating that uric acid will be added to this plate. One mL of media was removed from each well in the 'Uric Acid' plate and was replaced with 1 mL of 38 mg/dL uric acid solution prepared also in DMEM medium. To mimic bacterial infection process and to stimulate macrophages, formalin-fixed bacteria (150 µl per well) were added to designated wells in each plate. The following bacteria were used *S. aureus* (**SA**), low level Methicillin resistant *S. aureus* (MRSA-**LR**) and high level resistance *S. aureus* MRSA-**HR,** sensitive *Klebsiella pneumoniae* (**KPS**) and resistant *K. pneumoniae* (**KPR**). 150 µL of bacterial suspensions adjusted to OD 3 of each bacterial type were added into designated wells. Unstimulated cells in each plate were used as a negative control. Figure 3-1 represents the 6-well plate template followed across experiments.

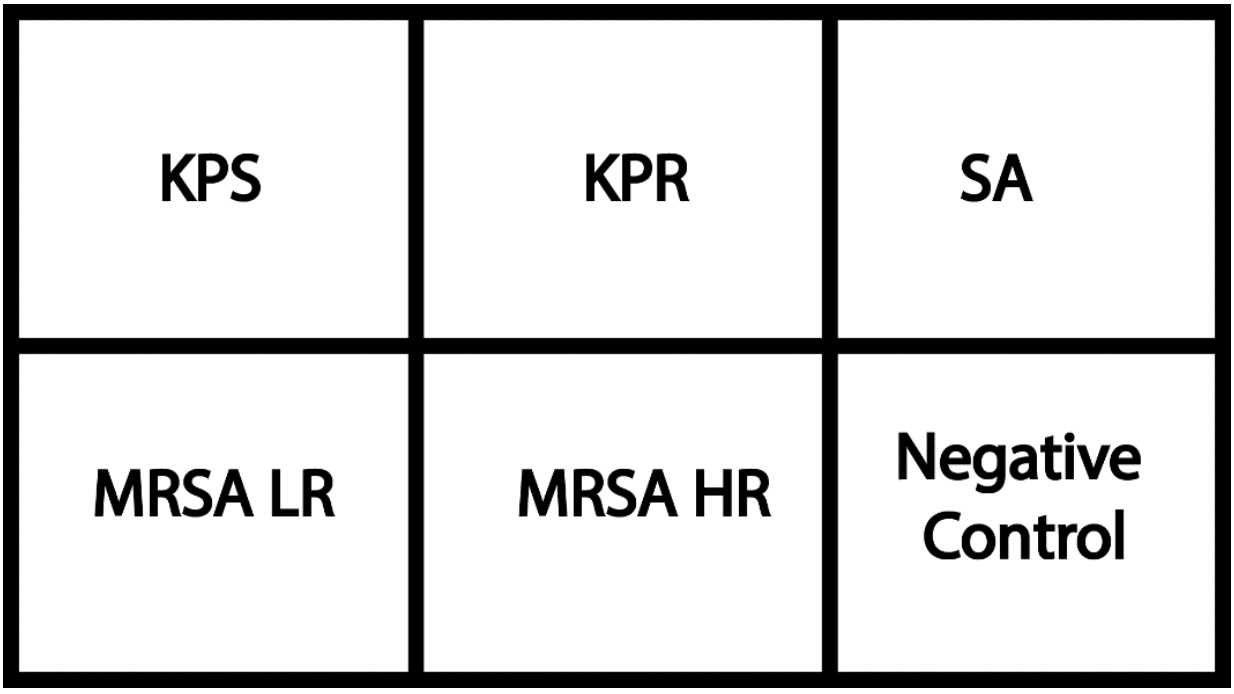

Figure 3-1 6-well plate template that was followed across experiments.

Each well contained a single coverslip with the designated bacterial type. Half plates were treated with uric acid while the other half did not.
KPS: *K. pneumoniae* sensitive; KPR: *K. pneumoniae* resistant; SA: *S. aureus*; MRSA LR: methicillin resistant *S. aureus* Low Resistance; MRSA HR: Methicillin Resistant *S. aureus* High Resistance.

3.7.2 Macrophage preparation and induction in 96-well plate

RAW264 cells were used in 96-well plates. Cell counts were adjusted to 270,000 cells per well. A template using 2-fold dilutions starting from 70 µL of each type of OD 3 formalin fixed bacteria in duplicate wells were used (Figure 3-2). The dilutions ranged from 70 µL to 4.375 µL for each type of bacteria as mentioned above, with and without uric acid. The amount of uric acid used was equivalent to 19 mg/dL per well. The last two rows in the 96-well plates were dedicated for negative controls.

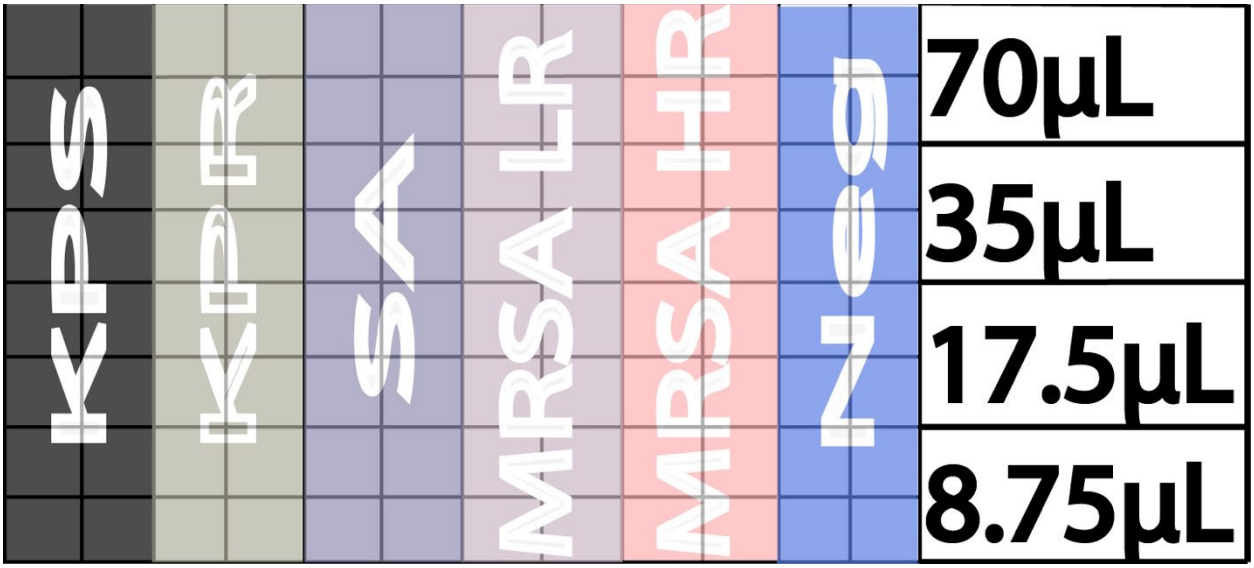

Figure 3-2 A 96-well plate template that was followed across experiments.

Number on the right side represent the concentration of bacteria in each well. Samples were run in duplicates.
KPS: *K. pneumoniae* sensitive; KPR: *K. pneumoniae* resistant; SA: *S. aureus*; MRSA LR: methicillin resistant *S. aureus* Low Resistance; MRSA HR: Methicillin Resistant *S. aureus* High Resistance.

A total of four 6-well plates, and two 96-well plates were prepared for each experiment (including technical duplicates), which were then incubated at 37ºC with 5% (v/v) CO_2 overnight. Next day, 300µL of supernatant from each well in the 96-wells plates and 6-well plates were collected into clean 96-well plates and stored at -80ºC till further use for nitric oxide and -80ºC IL-1β analysis. Further, 1mL of supernatants from the 6-well plates were transferred into Eppendorf tubes and stored at -80ºC till further use. To prepare macrophages on coverslips in 6-well plate for staining, cells were washed twice with PBS, fixed with 1 mL 5% formalin for 30 minutes, and then stained with DAPI for 5 minutes incubation time in the dark.

3.8 DAPI preparation

DAPI was prepared by diluting the stock (2 mg) in 2 mL distilled water to yield a concentration of 5 mg/mL. Intermediate solution was prepared by adding 2.1 µL to 100 µL PBS, yielding a concentration of 300 µM. The stock was kept at -20ºC along with several Eppendorf tubes of prepared DAPI solution. Before use, DAPI was further diluted in PBS in a 1:1000 ratio to yield a concentration 300nM as staining concentration recommended by the manufacturer (ThermoFisher).

3.9 Confocal Microscopy Imaging and Image Analysis

Microscope slides were cleaned with Kim-Wipes and labelled with a labelling scheme similar to that of the 6-well plate. A drop of mount media (Slow Fade) was placed in the middle of each slide without bubbles. Coverslips from each well plate were gently lifted up using a small surgical knife then held carefully to release excess moisture by placing them in a vertical position relative to a Kim-Wipe laying horizontally on the bench. Following that, coverslips were placed over the mount media on glass slide with the face containing the cells directed towards the slide. Pressure is applied gently by pressing Kim-Wipes against the surface of the slide to remove excess mounting media. Once excess media was removed, coverslips are sealed with nail polish and are imaged using Olympus Fluoview FV3000 confocal microscope. Since macrophages were stably transfected with a GFP-LC3 tag, the FITC and DAPI channels were used to visualize autophagy induction and capture images. Autophagy induction was assessed by taking several images from different fields (at least 1 image of 1 field of each coverslip). The images obtained were then analyzed using Image J software. The software was used to calculate autophagy index by defining regions of interest (ROI) across all fields and calculating the

intensity of GFP-LC3 and dividing it by the intensity of DAPI. Hence, it is possible to normalize autophagosomes puncta (represented by intensity of GFP) to the number of cells (represented by the intensity of DAPI). This allows for the comparison of the strength of autophagy between different cells undergoing different treatments.

3.10 Griess Assay for Nitric Oxide Quantification

Griess assay was used to determine the amount of nitric oxide produced by RAW264 cells as previously described (Zughaier Infection and Immunity 2004). Briefly, 1% sulfonamide was prepared by dissolving 0.5 gram of sulfonamide in 50 mL 1% orthophosphoric acid. 0.1 % N-(1-Naphthylethylenediamine) dihydride was prepared by dissolving 0.05 gram of 0.1% N-(1-Naphthylethylenediamine) dihydride in 50 mL of distilled water. Reagents were vortexed until they completely dissolved. Both reagents were stored in separate containers at 4^{o}C in the dark (wrapped in aluminum foil). Nitric oxide was measured in supernatants collected from RAW264 from 96-well plate induction and GFPLC3-RAW264 from 6-well plates as detailed above. 100 µL of supernatants was add to each well of a clean 96-well plate. Serial dilutions of standard were prepared by adding 100 µL of DMEM media in each well designated for standards. The first well has 10 µL of standard per 190 µL of media. The concentrations of standards used were 100, 50, 25, 12.5, 6.25, 3.125, 1.563, 0.781, 0.391, 0.195 µM of $NaNO_2$. Griess reagent was freshly prepared by mixing equal volumes 1:1 of 1% sulfonamide and 0.1% N-(1-Naphthylethylenediamine) dihydride. 100 µL of Griess reagent was added to each well and incubated for 5 min at room temperature. Each plate had four blanks containing DMEM media and Griess reagent only. Results were immediately read using Tecan plate reader infinite m200 pro at 540 nm wavelength. Standard curve and sample concentrations were obtained using ELISA-Analysis online software, while data analysis was done using Excel.

3.11 Mouse IL-1β Detection and Quantification

IL-1β was measured using the DueSet mouse IL-1β (mIL-1β) ELISA kit which provides required capture and detection antibodies as well as the streptavidin conjugate enzyme but not pre-coated plates, thus manually prepared and coated plates for ELISA. First, stock capture antibodies were reconstituted by diluting the content of the capture antibodies vial in 0.5mL PBS. 100 µL from the capture antibody stock is diluted in 10.5mL (per plate) PBS and vortexed well. 96-well pates were coated by adding 100 µL of the diluted capture antibody to each well. The plate was covered with parafilm and kept at room temperature overnight. Blocking reagent was prepared by adding 1g BSA to 100mL PBS to yield a concentration of 1% BSA in PBS. Next day, capture antibodies were removed from the plate by quickly flipping the plate in the sink and tapping it against clean tissue paper. 270 µL of blocking reagent was then added into each well of each plate using a multichannel pipette and the plates were covered and placed at room temperature for two hours. While incubating, recombinant mouse IL-1β standards were prepared by adding 0.5mL filtered 1% BSA to the lyophilized standards vial. Dilution of the standard was then prepared by adding 16 µL from the standard stock to an eppendorf containing 1 ml of 1% BSA to yield a starting concentration of 1000 pg/mL. Seven 2-fold dilutions were performed to prepare seven standards ranging in concentration from 1000 pg/mL to 15.635 pg/mL. In addition, 100 µL of each sample was transferred from either sample Eppendorf or 96-well plates (both moved to 4ºC one day before ELISA preparation to allow the samples to thaw slowly) to new 96-well plates and templates are made. 100 µL of each standard was added to wells 1 through 7 in duplicates rows (A and B). Wells 8-10 were used for samples and wells 11 and 12 were used as blank (100 µL 1% BSA). 100 µL of each sample was added to the new 96-

well plate (C through H) in duplicates along with the standards. After incubation, the plates were flipped and tapped against clean tissue paper to remove the blocking reagent and the content of the sample/standards containing 96-well plate is transferred to the ELISA plate. The sample and standards were covered and incubated for two hours. While waiting, biotinylated antibody was prepared by adding 1ml of 1% BSA to the detection antibody vial. From the biotinylated stock, 180 µL is diluted in 10.5 mL 1% BSA for each 96-well plate. After 2 hours, ELISA plates were washed twice with PBS with flipping and tapping after each wash. After washing, 100 µL of diluted biotinylated antibodies were added to each well in each plate. Plates are covered and incubated at room temperature for two hours or stored at 4^{o}C overnight. Streptavidin-HRP only requires dilution. 250 µL of Streptavidin-HRP (conjugate enzyme antibody) was diluted in 10.5 mL 1% BSA per each 96-well plate and stored in the dark. Biotinylated antibodies were removed from the plates by flipping and tapping. Plates were washed twice with PBS. 100 µL of diluted streptavidin-HRP was added to each well, plates were covered and incubated in the dark for 20 minutes. During 20 minutes of incubation, the substrate is prepared by mixing equal amount of substrate A and substrate B (5.4 each per plate). After 20 minutes incubation, plates are washed twice with PBS. 100 µL of substrate mixture is then added to each well for another 20 minutes. The reaction is stopped after the incubation with 50 µL of 2N sulfuric acid. Plates were read within 5-10 minutes using Tecan plate reader at a wavelength of 450 nm and a reference wavelength of 570 nm.

3.12 Autophagy Flux

RAW 264.7 macrophages devoid of any GFP-tag were used to investigate autophagy flux in stimulated macrophages in presence and absence of uric acid. 6-well tissue culture pates with coverslips were prepared in a similar manner as mentioned earlier in the macrophage induction

section. However, rapamycin, the chemical autophagy inducer, and LPS a potent inducer of autophagy, were used as the positive control were included in this experiment. Lyophilized Rapamycin was resuspended in 50 µL DMSO to prepare a stock solution. From the stock solution, rapamycin was diluted by a factor of 1:1000 in a single well containing known concentration of media. Following that, 50 µL of 1 nM LPS was added to different well as a second positive control for autophagy. A total of three 6-well plates induced with formalin fixed bacteria, positive controls, and treated with or without uric acid were incubated overnight in the tissue culture incubator. Next day, 1 mL supernatant was collected from each well and stored at -80^{o}C to be later used for IL-1β and nitric oxide analysis. In addition, 100 µL from each well in the 6-well plates were added to a clean 96-well plate for indirect nitric oxide quantification which was performed as described in the Griess reaction section. Culture media was removed from all the 6-well plates, and each plate was washed twice with 2 mL phosphate buffered saline. Washed cells were incubated with 1 mL of DMEM media without phenol red supplemented with 5% FBS. Staining reagent from the Cyto-ID Autophagy Flux (Enzo) detection kit was prepared by mixing 2 µL of the Green detection reagent with 1 µL Hoechst nuclear stain in 1 mL of DMEM media without phenol red supplemented with 5% FBS. Sufficient quantity of detection reagent was prepared, and 1 mL was added into each well. Plates were covered with foil and incubated at 37^{o}C for 30 minutes. After 30 minutes, detection reagent was discarded, and plates were washed twice with 2 mL PBS-FBS. Cells were fixed in 1 mL of 5% formalin for 20 minutes. Slides for confocal microscopy imaging were prepared as described above in the confocal microscopy and image analysis section. ELISA for the quantification of IL-1β in the harvested supernatants was performed as described in the IL-1β detection and quantification assay section.

3.13 Statistical Analysis

Statistical analysis was done using Microsoft Excel and reassessed using GraphPad Prism software. Student t-test followed by One-way ANOVA analysis were conducted. P values less than 0.05 were considered significant.

4. Results

4.1 Autophagy Flux Induction in Macrophages

Autophagy is a homeostatic process involved in cellular macromolecules recycling. Autophagy is also a host defense mechanism as it facilitates pathogen clearance (125). Further, autophagy is considered an anti-inflammatory process that dampens and regulates immune responses (142). The modulation of autophagy during cellular perturbations in macrophages such as pathogen invasion or inflammatory trigger, determines the outcome of this interaction. Specifically, autophagy induction during infection and inflammation leads to the resolution of inflammation and clearance of infection. Endogenous inflammatory stimuli such as uric acid are known to induce sterile inflammation. For example, uric acid crystals induce gouty arthritis, whereas hyperuricemia is associated with many inflammatory chronic diseases such as diabetes, cardiovascular diseases, and kidney disease (112, 143). Individual with chronic diseases usually have immune suppression and therefore are more prone to infections. The goal of our study is to investigate the role of uric acid as endogenous inflammatory stimuli on the ability of macrophages to induce autophagy during bacterial infection. Specifically, we investigated autophagy induction in macrophages infected with clinically relevant bacterial strains representing Gram-negative and Gram-positive bacteria in presence and absence of uric acid. We observed that bacterial infection induced autophagy flux in macrophages and that response is enhanced in presence of uric acid (Figure 4-1). In addition, inflammatory response was prominent with Gram-negative bacteria in contrast to Gram-positive bacteria and the presence of uric acid reduced this response.

To test for the effect of sterile and septic inflammation on autophagy, autophagy flux studies were performed using the autophagy detection kit on RAW 264.7 macrophages

stimulated using different strains of *S. aureus* and *K. pneumoniae* in the presence and absence of uric acid co-stimulation. Figure 4-1 shows representative images taken from twelve different stimulation conditions. Visual comparison between the bacterial induced cells and cells co-stimulated with uric acid and bacteria exhibit increased number of green puncta. These puncta reflect the fact that uric acid increases the process of autophagy. To confirm this, quantitative analysis to measure the fluorescence intensity of each stimulation condition was performed.

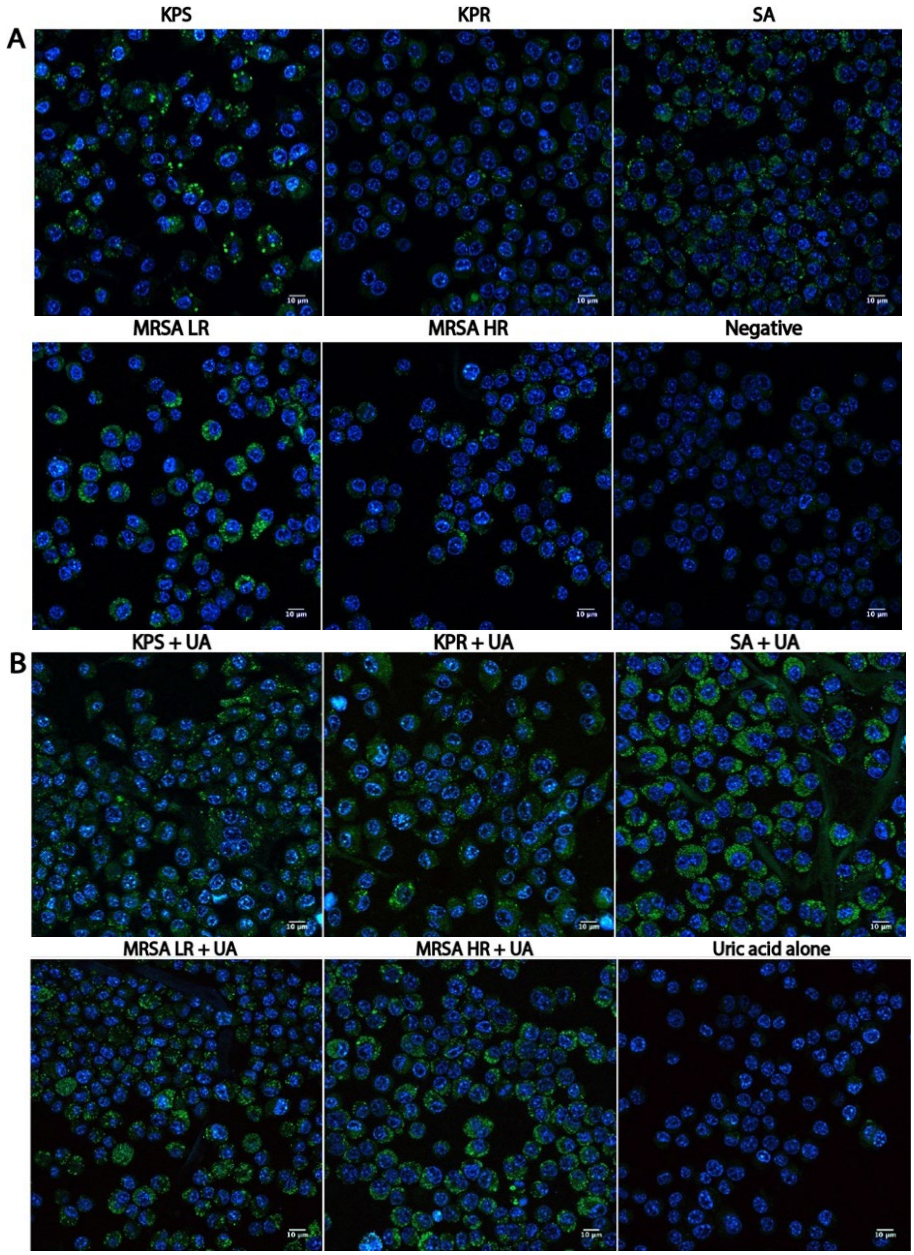

Figure 4-1 Autophagy flux images of RAW 264.7 macrophages.

Representative images of murine RAW 264.7 macrophages induced with different strains of *S. aureus* and *K. pneumoniae* and stained with Autophagy flux detection using autophagy flux kit. A) Macrophages induced with bacteria only. B) Macrophages induced with bacteria and uric acid (19 mg/dL) of. Nucleus is shown in blue color, and active autophagy is seen as green puncta. KPS: *K. pneumoniae* sensitive; KPR: *K. pneumoniae* resistant; SA: *S. aureus*; MRSA LR: methicillin resistant *S. aureus* Low Resistance; MRSA HR: Methicillin Resistant *S. aureus* High Resistance; UA: Uric Acid.

In order to systematically quantify the amount of autophagy induction in these images, ImageJ software for image analysis was used to calculate GFP/DAPI ratio across all images using multiple images from each condition. Figure 4-2 was created using GraphPad Prism software. There is no significant difference between *K. pneumoniae* strains and *S. aureus* strains in terms of autophagy flux induction. However, *S. aureus* the sensitive strain showed the highest levels of autophagy flux induction with and without uric acid. When macrophages were co-stimulated with uric acid and bacteria, autophagy flux increased but the increase was not significant between induction with bacteria alone and co-induction with uric acid and bacteria. There was a significant difference in GFP/DAPI ratio between co-stimulation with *S. aureus* and *K. pneumoniae* the sensitive strain. However, when *K. pneumoniae* resistant strain was compared with *S. aureus* the difference is not significant. The response of RAW 264.7 macrophages to co-stimulation with uric acid in the two types of bacteria is different. Specifically, GFP/DAPI ratio in images taken from co-stimulation with uric acid and the three different strains of *S. aureus* seem to be much higher than when bacteria alone are used. Despite finding a similar pattern in the case of *K. pneumoniae*, the presence of uric acid seems to lead to a less profound increase in GFP/DAPI ratio.

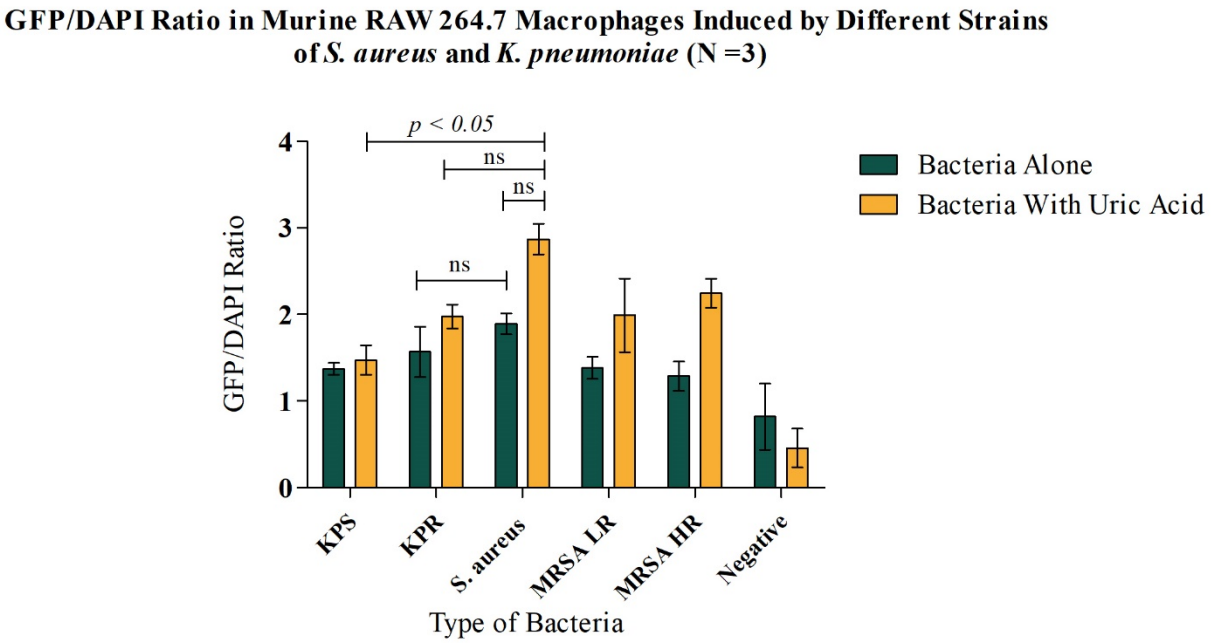

Figure 4-2 Quantitative analysis of confocal microscopy images

Autophagy flux quantitation using the intensity of GFP to DAPI ratio calculated in murine RAW 264.7 macrophages induced by different strains of *S. aureus* and *K. pneumoniae* in presence and absence of uric acid stimulation (19 mg/dL). The data represent the mean of three independent experiments with error bars depicting the standard error of the mean. The images were analyzed using ImageJ analysis software. Values $p < 0.05$ were considered to be significant. KPS: *K. pneumoniae* sensitive; KPR: *K. pneumoniae* resistant; SA: *S. aureus*; MRSA LR: methicillin resistant *S. aureus* Low Resistance; MRSA HR: Methicillin Resistant *S. aureus* High Resistance; UA: Uric Acid; ns: not-significant

4.2 Inflammation and Autophagy Cross-talk in Macrophages

Since autophagy induction in macrophages is considered an anti-inflammatory process, we investigated the impact of autophagy flux induction in infected macrophages on the levels of production of the pro-inflammatory cytokine IL-1β. Several studies established the link between autophagy induction and pro-inflammatory cytokines suppression and degradation (7, 142, 144). IL-1β is a critical pro-inflammatory cytokine that plays a critical role during bacterial infection

since it induces fever, hence named leukocytic pyrogen, it also affects cellular proliferation and differentiation (145, 146). IL-1β is produced in large quantities via the NLRP3 inflammasome activation that leads to production of the pro-IL-1β form which then is cleaved by capsase-1 to yield the mature and secreted IL-1β form (147). Pathogen associated molecular patterns (PAMP) such as LPS, peptidoglycan, lipoteichoic acid, DNA and bacterial membrane lipoproteins are known to induce IL-1β production in macrophages. Moreover, danger associated molecular patterns (DAMP) such as soluble uric acid and uric acid crystals are also induce IL-1β production (148, 149). Therefore, inflammasome activation and consequent IL-1β production is an important determinant of host defense responses and pathogen clearance.

4.3 Cytokine Studies

4.3.1 Single Dose IL-1β production

The production of the pro-inflammatory cytokine IL-1β from murine RAW 264.7 macrophages was investigated using ELISA method to quantify the secreted mature IL-β form in the supernatants collected 18-20 hrs after infection in presence and absence of uric acid. Different bacterial strains were used in this study to examine autophagy flux in macrophages. Therefore, to eliminate the differences and effects of live bacterial infection in macrophages we used inactivated whole cell formalin-fixed bacteria which eliminated the effect of secreted bacterial virulence factors during infection in macrophages. The use of formalin-fixed whole cell bacteria preserves the shape, bacterial surfaces and membrane structures to make it biological mimics of Gram-positive and Gram-negative bacteria that are not capable of killing macrophages. Thus, we used inactivated bacteria to induce autophagy and monitor immune responses such as IL-1β release.

IL-1β production by RAW 264.7 macrophages infected with different bacterial strains was compared in supernatants using ELISA method. Macrophages were infected using the same dose of each bacterial strain in presence or absence of uric acid in 6-well tissue culture plates (150 µL of OD = 3 bacteria in 2 mL of media). The data indicate that the Gram-negative bacteria *K. pneumoniae* induced the production of significantly higher amounts of IL-1β compared to Gram-positive *S. aureus* strains (Figure 4-3). Furthermore, there was a decrease in IL-1β production in the presence of uric acid amongst all types of bacteria. However, this reduction was not significant. Interestingly, IL-1β production under both conditions was significantly higher ($p < 0.05$) in *K. pneumoniae* sensitive and *K. pneumoniae* resistant in comparison to the three different strains of *S. aureus* which produced little to no detectable amounts of IL-1β. In the case of *S. aureus* MRSA HR resistant strain, detectable amounts of IL-1β under both conditions was not observed.

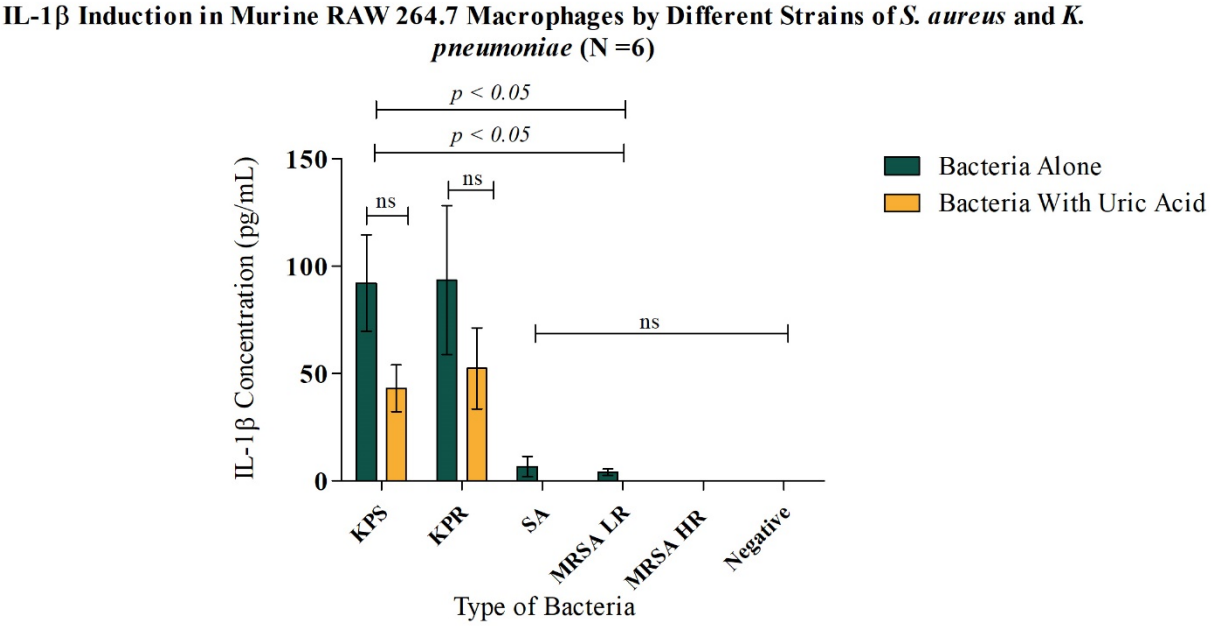

Figure 4-3 Quantitation of IL-1β under different treatment conditions.

This data represents the mean of six independent experiment with bars showing the standard error of the mean. The graph shows RAW264 macrophages production of IL-1β upon stimulation by inactivated formalin-fixed bacteria: KPS, KPR, SA, MRSA LR, and MRSA HR. The same concentration of bacteria was used in all experiments. Uric acid attenuated the response of macrophages and decreased the IL-1β production in all types of cells There was a significant difference between KPS and KPR and the three strains of *S. aureus* in terms of IL-1β production. KPS: *K. pneumoniae* sensitive; KPR: *K. pneumoniae* resistant; SA: *S. aureus*; MRSA LR: methicillin resistant *S. aureus* Low Resistance; MRSA HR: Methicillin Resistant *S. aureus* High Resistance; UA: Uric Acid.

4.3.2 Dose-Response IL-1β Production

Dose response relationship between bacterial concentration and IL-1β production was studied by performing two-fold dilutions on each type of bacteria all adjusted to equal density of OD = 3 as detailed in Methods section. Different concentrations were used: 70, 35, 17.5, and 8.75 µL of each bacterial strain which were further diluted into a total volume of 270 µL. The data suggest that the Gram-negative bacteria *K. pneumoinae* induced IL-1β production in a dose-dependent manner (Figure 4-4). Whereas, the Gram-positive bacteria i.e. all strains of *S. aureus*

(*S. aureus* sensitive, MRSA low resistance, and MRSA high resistance) did not show any detectable amounts of IL-1β production at any concentration even with co-stimulation with uric acid (19 mg/dL). Thus, a dose response relationship could not be determined for either condition (with or without uric acid). In contrast, *K. pneumoniae* induced macrophages to produce quantifiable amounts of IL-1β as demonstrated in Figure 4-4. Increasing the bacterial dose in the case of *K. pneumoniae* lead to an increase in IL-1β concentration indicating increase in macrophage activation. However, at 70 μL the increase becomes more subtle in *K. pneumoniae* sensitive and non-existent in *K. pneumoniae* resistant strain. Where resistant *K. pneumoniae* sometimes shows a slight decrease in IL-1β production at 70 μL of bacteria in comparison to IL-1β concentration at 35 μL. This observation is true for both stimulation with bacteria alone and stimulation with bacteria and uric acid. Further, the data demonstrate that the presence of uric acid decreased the production of IL-1β at all concentrations of bacteria. Although data illustrated in graph shows comparable results for IL-1β in the presence and absence of uric acid at high bacterial concentration of 70 μL, results from other experiments (not shown) indicated a slight decrease in IL-1β production in the presence of uric acid at the same concentration.

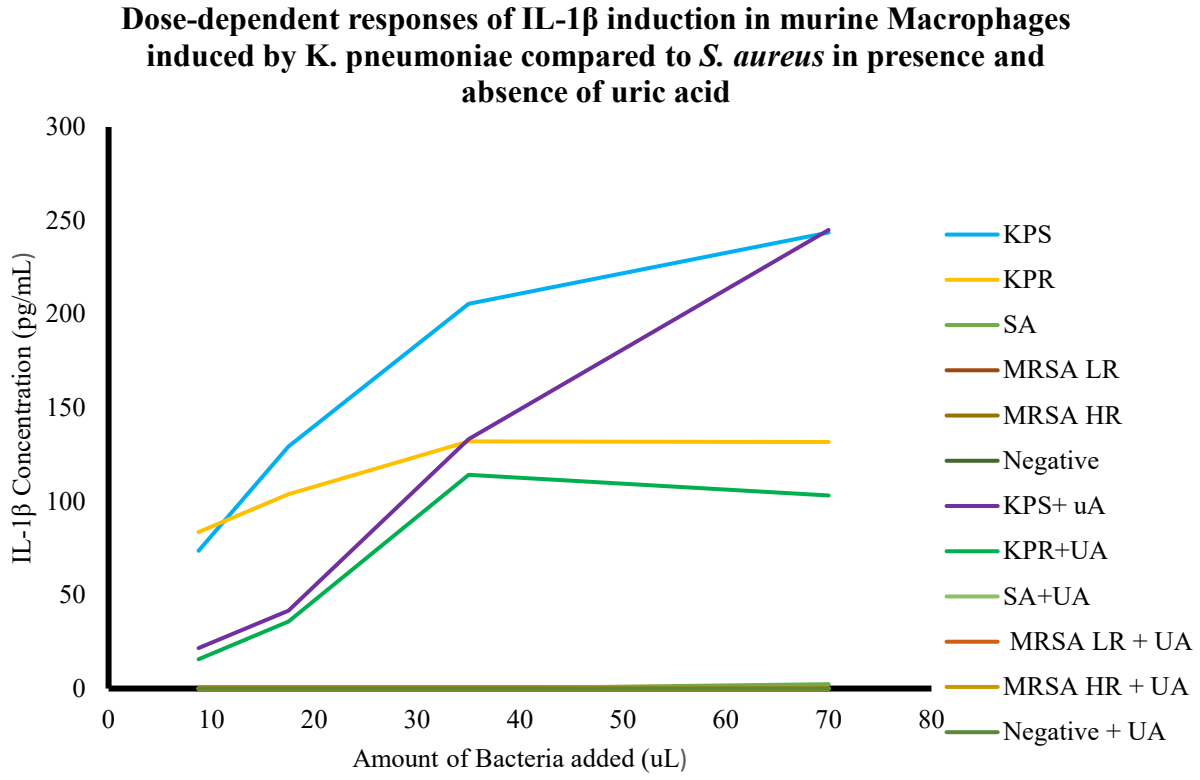

Figure 4-4 IL-1β dose-response curve

A representative graph of N = 6 of the dose response relationship between bacterial concentration and IL-1β production by murine macrophages RAW 264. Increasing concentrations of *Klebsiella* KPS and KPR increased IL-1β production. The three Gram-positive strains of *S. aureus* showed little to no response with regards to IL-1β at all concentrations with or without uric acid. KPS: *K. pneumoniae* sensitive; KPR: *K. pneumoniae* resistant; SA: *S. aureus*; MRSA LR: methicillin resistant *S. aureus* Low Resistance; MRSA HR: Methicillin Resistant *S. aureus* High Resistance; UA: Uric Acid.

4.4 Nitric Oxide Determination Using the Griess Reaction

Nitric oxide (NO) is small molecule produced by many cell types and plays important role in cellular responses during homeostasis and perturbations such as infection. NO is reported to inhibit inflammasome activation and reduces IL-1β release (150). Inflammasome is involved in host defense and bacterial clearance, however uncontrolled inflammasome activation leads to

disease and inability to resolve inflammation or infection. For example, nitric oxide is often found elevated in patients with gouty arthritis characterized by uric acid crystals precipitating in the joints (151).

We monitored nitric oxide release as another inflammatory molecule produced by macrophages during stimulation using Griess reaction, which is an indirect quantification method of nitric oxide production that detects accumulated nitrites in supernatants of infected macrophages (152). Nitric oxide production by murine macrophages 264.7 was assayed in a similar manner to that of IL-1β using two methods. Firstly, RAW 264.7 macrophages were infected with a single concentration of bacteria (150 µL of OD = 3 bacteria in 2 mL of media) in the presence or absence of 19 mg/dL uric acid (Figure 4-5). Secondly, dose dependent production of NO was measured in infected macrophages RWA 264.7 in the presence or absence of uric acid (Figure 4-6-A and Figure 4-6-B).

To this end, Figure 4-5 shows a comparison of nitric oxide production from RAW264 induced by different bacterial strains with or without uric acid. The results of nitric oxide production are similar to those of IL-1β production in which there was a significant difference ($p < 0.05$) between the Gram-negative bacteria *K. pneumoniae* sensitive and resistant strains and the three different Gram-positive strains of *S. aureus* (Figure 4-5). However, co-stimulation of cells with formalin-fixed bacteria and uric acid showed slightly higher levels of nitric oxide production in all types of bacteria except *S. aureus* sensitive where it showed a slight decrease in nitric oxide production. Despite those difference, uric acid showed no significant effect on nitric oxide production by murine macrophages RAW 264.7 in the presence of different strains of formalin-fixed S. *aureus* and *K. pneumoniae*.

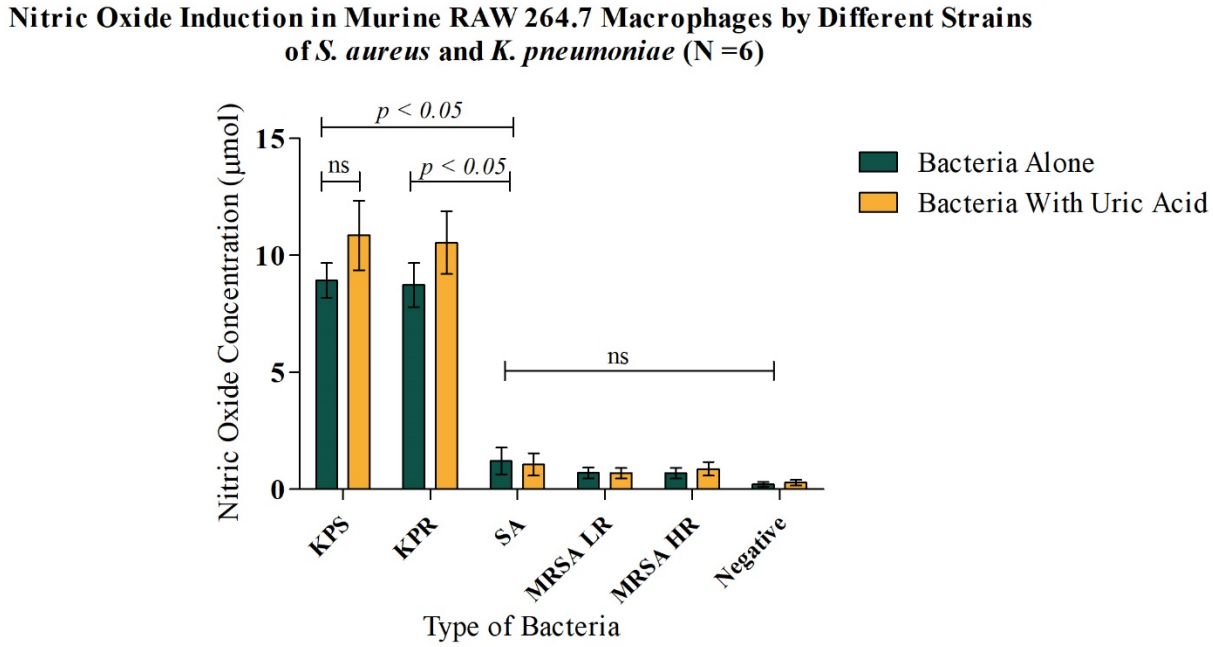

Figure 4-5 Quantitation of nitric oxide under different treatment conditions.

Nitric oxide production data represent the mean of six independent experiments with bars showing the standard error of the mean. The graph shows RAW264 macrophages production of nitric oxide upon stimulation by formalin-fixed killed bacteria: KPS, KPR, SA, MRSA LR, and MRSA HR. The same concentration of bacteria was used in all experiments. Uric acid increased nitric oxide production in KPS and KPR but the increase is not significant. The differences in nitric oxide production with and without uric acid in SA, MRSA LR, and MRSA HR are variable. In SA there was a slight decrease in nitric oxide production, MRSA LR shows no difference, and MRSA HR shows an increase in nitric oxide production. There is a significant difference between KPS and KPR and the three strains of *S. aureus* in terms of nitric oxide production. KPS: *K. pneumoniae* sensitive; KPR: *K. pneumoniae* resistant; SA: *S. aureus*; MRSA LR: methicillin resistant *S. aureus* Low Resistance; MRSA HR: Methicillin Resistant *S. aureus* High Resistance; UA: Uric Acid.

Furthermore, a dose response relationship of bacterial concentration and nitric oxide production was studied and two dose response graphs were generated and are depicted in Figure 4-6-A and 4-6-B. The data presented in Figure 4-6-A, indicate that *S. aureus* sensitive (SA) induced a dose-dependent nitric oxide release and co-stimulation with uric acid led to a decrease in nitric oxide production at all concentrations (Figure 4-6-A). In addition, MRSA LR and

MRSA HR produced less nitric oxide on general in comparison to sensitive *S. aureus* and the presence of uric acid resulted in a slight to no decrease in nitric oxide levels. On the other hand, Figure 4-6-B depicts nitric oxide production by *K. pneumoniae.* Both sensitive and resistant *K. pneumoniae* produced higher concentrations of nitric oxide at all doses in comparison to all strains of *S. aureus.* LPS present in Gram-negative bacteria is known to be a potent inducer of nitric oxide. Nitric oxide production appears to be consistent at all doses of bacteria, where the difference between one dose and another is 1 to 2 µM only. The presence of uric acid increase the production of nitric oxide by RAW 264.7 macrophages.

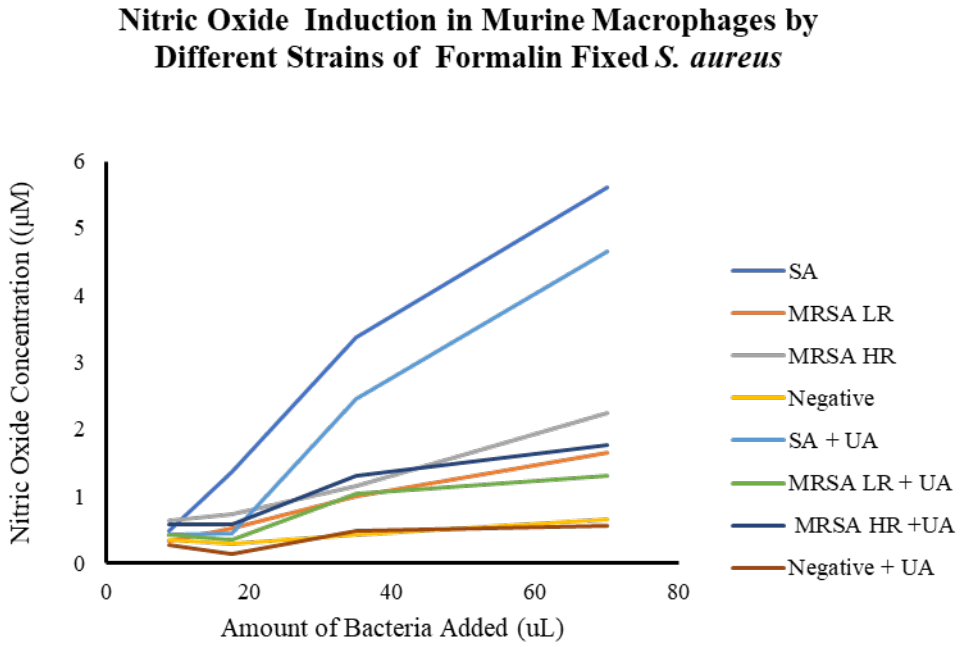

Figure 4-6-A Nitric oxide dose response curve with S. aureus

A representative graph of N = 6 of the dose response relationship between bacterial concentration and nitric oxide production by RAW-264 cells in the presence and absence of uric acid. SA: *S. aureus*; MRSA LR: methicillin resistant *S. aureus* Low Resistance; MRSA HR: Methicillin Resistant *S. aureus* High Resistance; UA: Uric Acid.

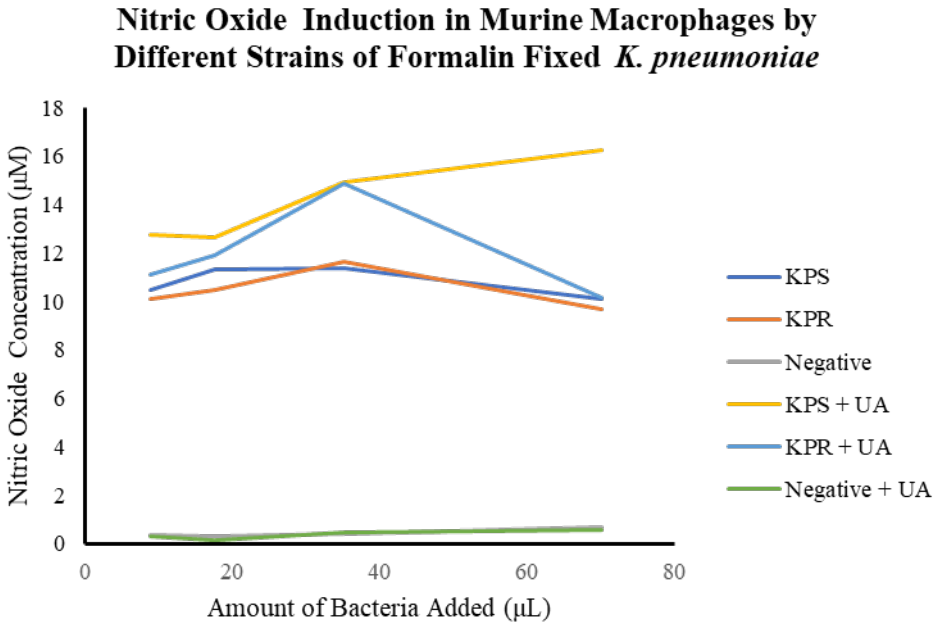

Figure 4-6-B Nitric oxide dose response curve with K. pneumoniae

A representative graph of N = 6 of the dose response relationship between bacterial concentration and nitric oxide production by RAW-264 cells in the presence and absence of uric acid. KPS: *K. pneumoniae* sensitive; KPR: *K. pneumoniae* resistant; UA: Uric Acid.

4.5 The Effect of Uric Acid and LPS on Macrophages

In order to validate the results of all experiments, various controls such as uric acid alone, LPS as well as unstimulated cells were used. The effect of uric acid alone without the addition of any stimulus was also studied in relation to the positive control (LPS) and the negative control. Three methods of comparison were used: Autophagy flux studies, nitric oxide measurements, and IL-1β quantification in supernatants.

Autophagy flux studies were performed on uric acid and LPS stimulated RAW 264.7 macrophages using Autophagy detection kit. Figure 4-7-A shows representative images taken by confocal microscope under these three conditions. Figure 4-7-B was created using ImageJ

analysis software to quantify GFP fluorescence and DAPI fluorescence. Ratios where obtained using Excel while graphs were obtained using GraphPad Prism software. Uric acid alone does not seem to exhibit a stimulating response to autophagy. The results of GFP/DAPI ratio show a decrease in autophagy in the presence of uric acid in comparison to the negative control. On the other hand, LPS, as a positive control, induces autophagy as expected.

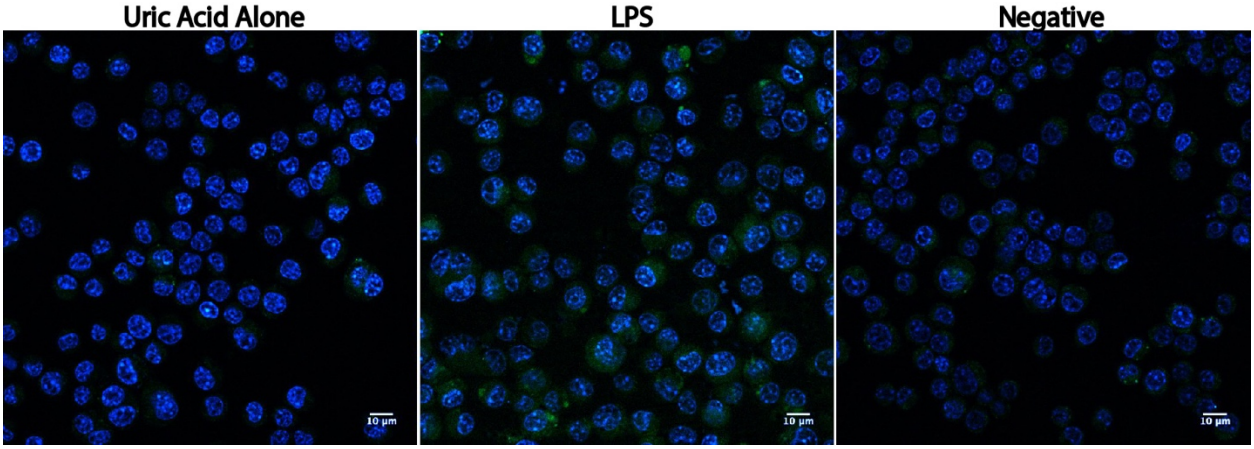

Figure 4-7-A Confocal microscopy images of experimental controls

Representative images of murine RAW 264.7 macrophages stained under three different conditions: stimulation with uric acid alone, LPS (10ng/ml), no stimulus. Autophagy flux is shown in these images using autophagy flux kit. Nucleus is shown in blue color, and active autophagy puncta are seen in green.

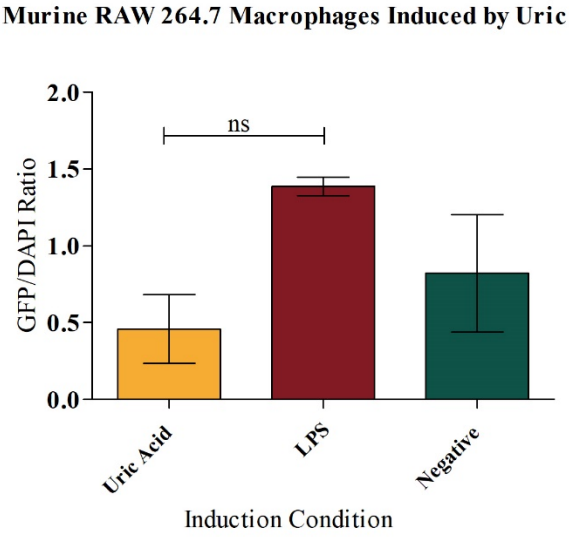

Figure 4-7-B Quantitative analysis of confocal images for experimental controls

A graph of GFP to DAPI ratio calculated in murine RAW 264.7 macrophages induced by uric acid and LPS. The data represents the mean of three independent experiments with bars showing the standard error of the mean. The images were analyzed using ImageJ analysis software. Values $p < 0.05$ were considered to be significant. Ns = not significant.

To further validate our results, we performed IL-1β and nitric oxide analysis on supernatants obtained from uric acid and LPS stimulated RAW 264.7 macrophages (Figure 4-7-C). When macrophages are stimulated with uric acid alone, they did not produce IL-1β or nitric oxide. LPS is a known stimulus for inflammatory process in macrophages, hence it produced notable levels of nitric oxide and IL-1β when used to stimulate macrophages. Furthermore, co-stimulation of macrophages with uric acid and LPS showed a decrease in nitric oxide production with an increase in IL-1β production when compared to stimulation with LPS alone.

IL-1β (N =1) and Nitric Oxide (N=5) Induction in Murine RAW 264.7 Macrophages by LPS and Uric Acid

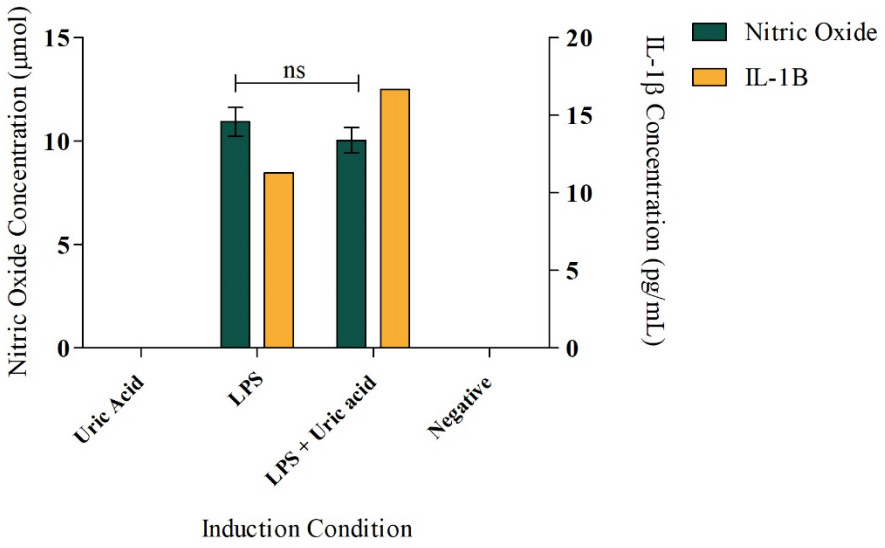

Figure 4-7-C Quantitation of IL-1β and nitric oxide for experimental controls

Graph representing IL-1β concentrations and nitric oxide concentrations in supernatants from murine macrophages 264.7 induced with LPS and uric acid. Data for nitric oxide represents two independent experiments while data from IL-1β shows results from one experiment.

5. Discussion

5.1 Autophagy flux is induced by co-stimulation of bacteria and soluble uric acid

Autophagy is a homeostatic mechanism that functions to maintain cellular integrity. It also plays a fundamental role in host defense mechanisms (125, 153). The inflammasome is a complex of proteins that work together to facilitate the release of the cytokines IL-1 and IL-18. There is an intricate interplay between autophagy and the inflammasome formation which leads to the subsequent release of inflammatory cytokines. Autophagy appears to act as an anti-inflammatory process by degrading damaged organelles and preventing the release of danger signals. Hence, autophagy is able to reduce the inflammasome activation as an immune regulatory process (154). This study examined the dynamics of autophagy and inflammation when mediated by soluble uric acid, formalin-fixed whole cell bacteria, or both in murine RAW 264.7 macrophages.

It is becoming widely accepted that *S. aureus* is able to infect non-phagocytic cells and act as an intracellular pathogen. It is hypothesized that *S. aureus* increases autophagy but halts autophagy flux in non-phagocytic host cells to facilitate its survival (155, 156). In addition, in phagocytic cells such as macrophages, phagocytosis as well as autophagy are both enhanced after *S. aureus* infection (157). When *S. aureus* is phagocytosed by the host cells, toxins produced by the bacteria (mainly α-toxin) disintegrate the phagosomal membrane. Autophagy is activated in an attempt to contain the cellular damage (158). However, it is worth to mention that *S. aureus* strains that do not disrupt the phagosomal membrane do not enhance autophagy in infected macrophage (159). There are no studies on the effect of formalin-fixed or heat killed inactivated *S. aureus* on the process of autophagy. Therefore, it is likely that the high autophagy

flux induced with *S. aureus* strains observed in our study herein is a result of toxins that remained inside the bacteria i.e. not secreted after formalin fixation. Moreover, since the bacteria were inactivated, hence their evading mechanisms were defective, autophagy was not halted, and active autophagy flux was also increased.

Regarding autophagy induction with Gram negative bacteria, there are fewer studies on autophagy induction during *K. pneumonia* infections. However, a study on alveolar macrophages demonstrated that autophagy is critical for effective and optimal clearance of *K. pneumoniae*. It is also worth to note that LPS alone and heat killed *K. pneumoniae* demonstrated an increase in autophagy, indicating that cellular or membrane components in live bacteria are the driving forces for autophagy activation (160). We found that both *S. aureus* and *K. pneumoniae* stimulate autophagy. However, induction with formalin-fixed *S. aureus* resulted in significantly higher autophagy activation compared to *K. pneumoniae*. This difference could be attributed to different types of toxins produced by the two types of bacteria and their effect on the phagosomal membrane since one is a model of Gram-positive bacteria while the other is represents Gram-negative bacteria. Nevertheless, infection with live bacteria to better mimic the effect of these two bacterial types on autophagy during infection in macrophages is warranted.

The relation between uric acid, whether soluble or in the form of MSU crystals, and autophagy in macrophages is poorly studied. Recently, Crişan *el. al.* demonstrated the effect of priming human macrophages with soluble uric acid. They observed a decrease in autophagy accompanied by an increase in IL-1 β, a common response to autophagy inhibition (161). Lack of autophagy and increase in proinflammatory IL-1β worsen the outcomes of subsequent exposure to an inflammatory stimuli in gout patients (161). Effect of MSU crystals on the other hand was not reported. Allaeys *et. Al* demonstrated that autophagy in osteoclast (non-

professional phagocytes) was enhanced as a result of NLRP3 activation without an increase in the production of IL-1β. Phagocytosis and mTOR downregulation were major contributors to the enhanced autophagy by MSU crystals (162). Whether these mechanisms of autophagy activation are applicable on murine macrophages remains to be elucidated. We demonstrated that co-induction of macrophages with uric acid and bacteria induced autophagy. This could be a result of the simultaneous stimulation of macrophage with both uric acid and bacteria, which excessively activated the cells and made them more sensitive to stimuli. In contrast, we also found that uric acid alone had inhibitory effects on autophagy, which is consistent with previous findings (161). Although we used soluble uric acid in our experiments, microcrystals of uric acid which appears as fine short needles are not always visible using light microscopy, might have been present and could be responsible for the results we are observing. These microcrystals would be poorly phagocytosed by macrophages alone (162), and the presence of bacteria would have probably enhanced their phagocytosis, thus enhancing the process of autophagy.

Nevertheless, the mechanism by which uric acid crystals activate autophagy has been described in the literature. Initially, uric acid crystals are phagocytosed by macrophages, due to the spindle structure of uric acid crystals, phagosomes rupture. Rupturing of phagosomes signals autophagy induction and activation (163). On the other hand, the mechanisms by which soluble uric acid activates autophagy has not been described in the literature. Interestingly, soluble uric acid activates the NLRP3 inflammasome, which is responsible for the production of IL-1β. However, uric acid alone is not enough to induce IL-1β. In our study, we found the co-stimulation of macrophages with both uric acid and bacteria led to the increase in IL-1β production. High levels of IL-1β levels are known to induce autophagy activation as a host defense response to prevent over activity of the inflammatory response (7). These findings are

consistent with the results we generated in our study, since co-stimulation of with bacteria and uric acid led to the increase in autophagy with a decrease in IL-1β production. However, when uric acid is used alone it inhibited autophagy. This effect could be explained by the paradoxical effect of uric acid as anti-oxidant and also as inflammatory and oxidant molecule in hyperuricemia (164).

5.2. IL-1 β increase during bacteria induction but decrease when macrophage are co-stimulated with bacteria uric acid

IL-1β is a proinflammatory cytokine that is regulated through a multiprotein structure known as the inflammasome. Cells produce pro-IL-1β in response to inflammatory stimuli. However, it is the caspase-1 activation by the inflammasome and the subsequent cleavage of pro-IL-1β to mature IL-1β that steers the inflammatory effects of this cytokine (142). In contrast to the activation of IL-1β by the inflammasome, autophagy inhibits the secretion of IL-1β. The control of IL-1β production is exerted in two ways; pro-IL-1β could be directly degraded by autophagy, or damage signals stimulating the inflammasome, such as those caused by ROS release after mitochondrial damage, could be sequestered and cleared through autophagolysosome formation (7, 165). The effect of bacterial induction, uric acid stimulation or co-stimulation of macrophages by bacteria and uric acid on the release of IL-1β, and hence on inflammation, was examined in this study.

During live bacterial infections toxins released during *S. aureus* infection result in the activation of the NLRP3 inflammasome the subsequent increase of IL-1β release (166-168). However, when using formalin-fixed *S. aureus* we found a decrease in IL-1β production. These observations could be due to easier clearing of bacteria by macrophages in their inactivated fixed

state, as well as inability of bacteria to actively produce toxins. Hence, they result in weaker inflammatory response. In addition, the great increase in autophagy during *S. aureus* induction could have contributed inhibitory effect on IL-1β release. *K. pneumoniae* surpluses the release of IL-1β through the activation of the NLRP3 inflammasome (169). A recent study found a capsular toxin in a *K. pneumoniae* strain that causes a massive increase in IL-1β levels through the formation of ROS and activation of the inflammasome (170). We found a significant difference between levels of production of IL-1β in *S. aureus* and *K. pneumoniae* which indicated that surface structures on bacteria are greatly responsible for IL-1β production. A study comparing *S. aureus* and *E. coli* demonstrated that *S. aureus* produced less IL-1β compared to *E. coli* (171). This could be the result of the activation of different receptors by Gram-positive versus Gram-negative bacteria, which activate TLR-2 and TLR-4 respectively (172, 173).

Uric acid in it soluble form is classified as a DAMP molecule that induces inflammation (174). Braga *et al.* reported that uric acid activates NLRP3 inflammasome through the stimulation of mitochondrial ROS formation leading to the consequent release of IL-1β. Despite that, uric acid alone is not capable of activating the inflammasome. Although it does increase the expression of pro-IL-1β. To activate the inflammasome, uric acid exposure must be followed by a second stimuli that facilitate the conversion of pro-IL-1β to mature IL-1β (149). Another study investigating the role of MSU crystals and the activation of the inflammasome in progressive multiple sclerosis also demonstrated an increase in the production of IL-1β (175). Whether inflammation is stimulated by soluble uric acid or MSU crystals, the end result is an increase in the release of IL-1β. There are no studies on the effect of simultaneous induction of macrophages using uric acid and bacteria on IL-1β production. In agreement with the literature, we report that uric acid alone does not cause the release of IL-1β. In addition, co-stimulation of macrophages

with LPS and uric acid increased IL-1β release compared to induction with LPS alone, which is what we hypothesized. On the other hand, we found that co-stimulation with bacteria and uric acid decreased the production IL-1β by murine RAW 264.7 macrophages. These results might have occurred because of the overwhelming effect of co-stimulation on macrophages which led to the exacerbation of autophagy, hence, inhibited the action of inflammasome and reduced IL-1β release. To add, if uric acid microcrystals were present, autophagy would increase, further explaining the decrease in IL-1β. Furthermore, heat killed *K. pneumoniae* seems to induce more autophagy in comparison to LPS from the same bacteria, again suggesting that the inhibition of IL-1β release is a result of autophagic regulation (160).

5.3 Nitric oxide release is induced by bacteria and uric acid

Nitric oxide is a gas molecule that is produced in response to various inflammatory stimuli, including LPS. Nitric oxide is highly unstable and degrades within few seconds after its release, generating nitrites (NO_2) and nitrates (NO_3) which are stable metabolites (176). Nitric oxide has a complex role in immune modulation. It could directly kill microbes, regulate immune cells, and modulate signaling cascades resulting in increased or decreased cytokine release (177). Nitric oxide is also known to inhibit both autophagy (9) and the NLRP3 inflammasome (178).

S. aureus infections increase nitric oxide production (179, 180). The increase of nitric oxide is due to the lipoproteins present in the bacterial surface which trigger nitric oxide synthase, the enzyme responsible for nitric oxide synthesis (181). In addition, nitric oxide release is stimulated by *K. pneumoniae* and is important for host survival (182). The induction of nitric oxide by both types of bacteria is similar and is mediated by the induced expression of nitric oxide synthase. The stimulation of nitric oxide occurs through the activation of nuclear factor

kappa B (NF-kB) pathway by bacterial surface antigens (183, 184). However, we found a significant increase in nitric oxide production by *K. pneumoniae* compared to that of *S. aureus*. This could be explained by the presence of LPS in Gram negative bacteria, which is the most potent TLR4 ligand, compared to other TLR ligands such as peptidoglycan, lipoteichoic acid, membrane lipoproteins and unmethylated DNA present in most bacteria. LPS therefore primes macrophages to produce more IL-1β and other immune responses. This also could be a due to the ability of IL-1β to induce nitric oxide production (185). As mention earlier, we observed increased IL-1β levels in the presence of *K. pneumoniae* but not in the presence of *S. aureus*, which in turn could explain the higher levels of nitric oxide seen in *K. pneumoniae* induction. It is worth to mention that NO production inhibits autophagy through mTOR and JKN pathways (9). This could further explain the activation of autophagy observed with *S. aureus* versus that of *K. pneumonia.*

High uric acid (hyperuricemia) in plasma downregulate nitric oxide by direct binding (186, 187).A study found that MSU crystals alone are unable to induce nitric oxide release. However, when cells were subjected to the cytokine IFN-gamma, a potent increase in nitric oxide was observed (188). Another study using RAW 264.7 macrophages showed that MSU crystals increased nitric oxide synthase in time and dose dependent manner through PI3K/Akt and NF-KB pathways (189). The use of extremely high dose of MSU crystals in this study might have resulted in enough stimulation to induce nitric oxide synthase without the help of a second stimulant. We observed that inducing macrophages with uric acid alone did not result in production of nitric oxide which is consistent with published studies. However, when uric acid was used in co-induction studies with bacteria, the levels of nitric oxide produced increased in comparison to infection with bacteria alone. This could also be attributed to excessive

stimulation of macrophage during co-infection. Furthermore, in case of the presence of undetected crystals and co-stimulation with bacteria could exhibit synergizing effect that may further activate TLR mediated release of nitric oxide (190). In agreement with literature, we found that co-stimulation of macrophages with LPS and uric acid reduced nitric oxide, however, contradicting the effect observed during bacterial induction. The discrepancies could be due to the use of formalin-fixed bacteria since phagocytosis of whole bacteria and the presence of membrane surface structures induced nitric oxide rather than inhibit it. Indeed, further investigations to optimize the experiments are required to unravel the mechanisms that control the effect of uric acid on autophagy, IL-1β release, and nitric oxide production.

6. Conclusion

To conclude, we reported the complex interplay between autophagy and the inflammasome during sterile and septic inflammation. The outcome of each condition is highly variable and depend of the specific circumstances of stimulation and induction microenvironment. Generally, whole cell formalin-fixed bacteria induce autophagy, which results in the degradation of the inflammatory cytokine IL-1β in case of *S. aureus* infection in contrast to *K. pneumoniae* infection. Moreover, nitric oxide release was increased during bacterial infection, which may have exerted synergistic effect with autophagy to further reduce IL-1β release during *S. aureus* infection. On the other hand, stimulatory signal by *K. pneumoniae* induced nitric oxide release. Uric acid increased autophagy and nitric oxide production while it reduced IL-1β release, suggesting an anti-inflammatory role of uric acid during septic infection. Much remains to be delineated to further understand the interplay of autophagy and the inflammasome during inflammation. Understanding the signaling cross-talk between autophagy and inflammasome will facilitate therapeutic target discovery and design.

Although the project has provided sufficient data and clearly drew the link between autophagy induction in sterile inflammation induced by hyperuricemia in comparison to inflammation induced by formalin-fixed bacteria. There were some limitations and challenges during the process of experimentation.

7. Challenges

Although we obtained GFP-LC3 RAW 264.7 macrophages cell line and used these macrophages in our experiments to quantify autophagy flux by observing co-localization of LC3 in the form of green puncta under fluorescent microscope. Imaging using confocal microscopy did not provide consistent quality of images. Most images had low quality and were not enough to be used in systemic image analysis to generate data using ImageJ analysis software. Representative images from these experiments are shown in Figure 9-1 in Appendix 1

To confirm the observations seen using GFP-LC3 RAW 264.7 macrophages and autophagy flux kit, we performed flow cytometry analysis on activated and infected macrophages using GFP quantification in those cells. However, we encountered an issue in setting the gating of the channels to differentiate between basal autophagy and autophagy flux puncta induced due to infection, cellular perturbation or simply starvation. Results from these experiments can be seen in Figure 9-2-A, 9-2-B, and 9-3 in Appendix 1.

The time allotted for the graduation project did not allow for solving GFP-LC3 RAW 264.7 confocal imaging issues nor to repeat those experiments and optimize flow cytometry gating. Further, optimizing other testing protocols such as determining optimal bacterial dose, optimizing uric acid preparation technique, Griess reaction, and IL-1β ELISA techniques test runs took longer than expected. Therefore, the initial project plan that included testing human THP-1 cells was postponed for now but planned for Summer along with confocal imaging and Flow cytometry analysis.

8. Limitations and Future Directions

The results of this study show that our model of sterile inflammation, hyperuricemia, inhibits autophagy without producing the inflammatory markers IL-1β or nitric oxide. However, when combined with formalin-fixed bacteria it induces autophagy and inhibits the production of IL-1β while increasing the production of nitric oxide. These findings are valuable since this paper is the first to investigate the interplay between autophagy and the inflammasome in the presence of two stimulus representing sterile inflammation and non-sterile inflammation.

However, the study presented with some limitations in the context of comprehensive coverage of all aspects of cellular interactions. Even though the murine macrophage cell lines are frequently used in autophagy studies, the interplay between autophagy induction and inflammation induced during sterile inflammation or bacterial infection should be further investigated in the context of human monocytic cell line THP-1, to recapitulate the observations studied in murine macrophages.

Furthermore, macrophage stimulation conditions under which our research was conducted did not mimic the normal pathological process, where the body is usually exposed to hyperuricemia for a duration of time, which then alters the body's response to invading pathogens. Therefore, future investigations will include a priming phase, where macrophages are incubated under hyperuricemic conditions for few hours before introducing bacteria as a secondary stimulus.

Killing bacteria using formalin allowed us to preserve the structure of the bacteria while preventing it from killing macrophages which allows for longer interaction time than during live infection. This approach allowed us to study the interaction of macrophages with surface receptors and structural components of both Gram-positive and Gram-negative bacteria.

However, this study shall move a step further and incorporate a cocktail of live infections accompanied with hyperuricemia or monosodium urate crystal induction which will provide a deeper insight on autophagy modulation during live infection and sterile inflammation.

9. Appendix 1

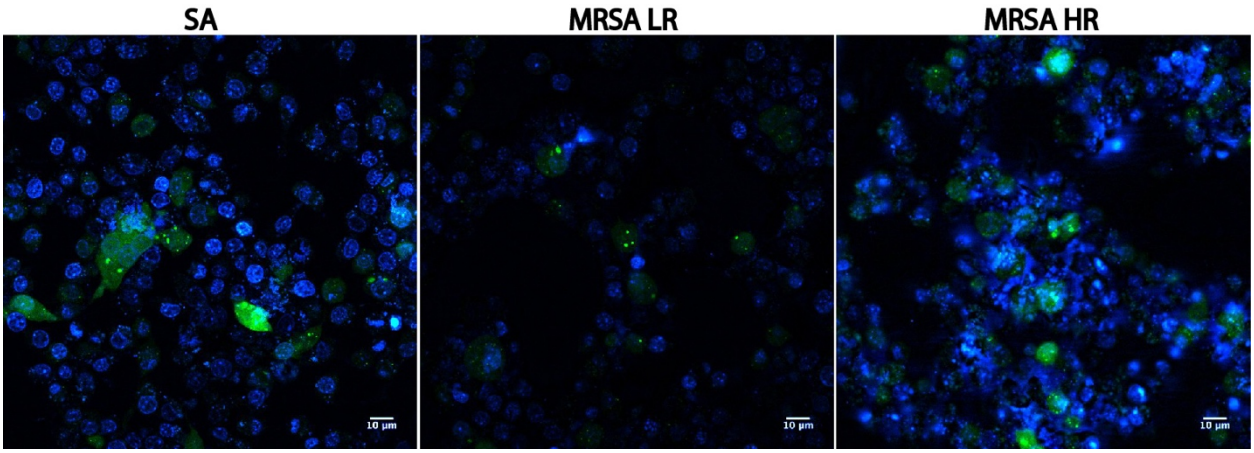

Figure 9-1 Confocal microscopy images of GFP-LC3-RAW 264.7 macrophages

Images obtained using GFP-LC3-RAW 264.7 cells line. As can be seen, the images are not of a consistent quality and they are blurred at times.
SA: *S. aureus Sensitive*; MRSA LR: methicillin resistant *S. aureus* Low Resistance; MRSA HR: Methicillin Resistant *S. aureus* High Resistance.

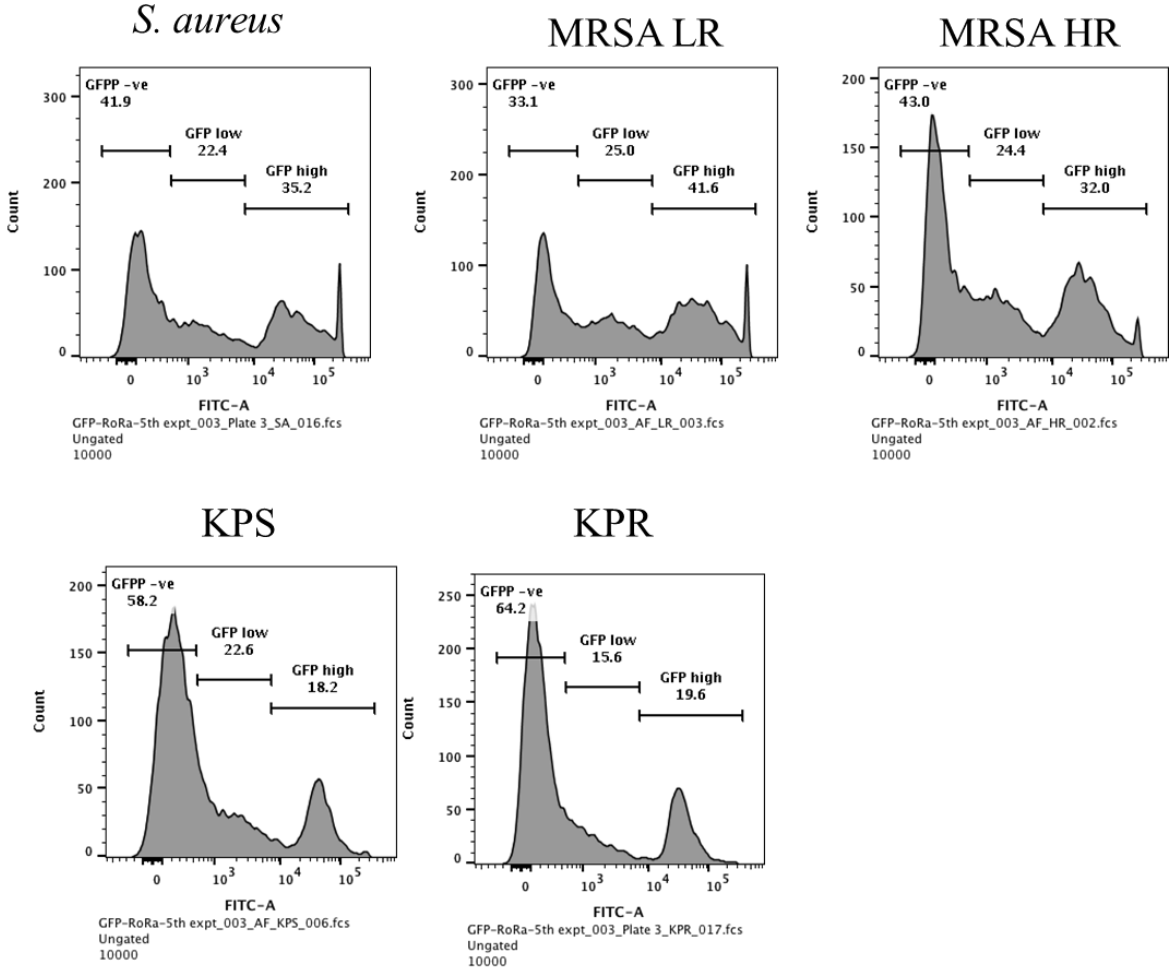

Figure 9-2-A Representative Flow-Cytometry Images for autophagy flux

Flow cytometry chart of autophagy flux cytoID studies showing the cell count versus fluorescence. The fluorescence intensity can be seen by the peak of the graph. Number of cells with GFP low, GFP high, and GFP negative can be seen.
KPS: *K. pneumoniae* sensitive; KPR: *K. pneumoniae* resistant; MRSA LR: methicillin resistant *S. aureus* Low Resistance; MRSA HR: Methicillin Resistant *S. aureus* High Resistance.

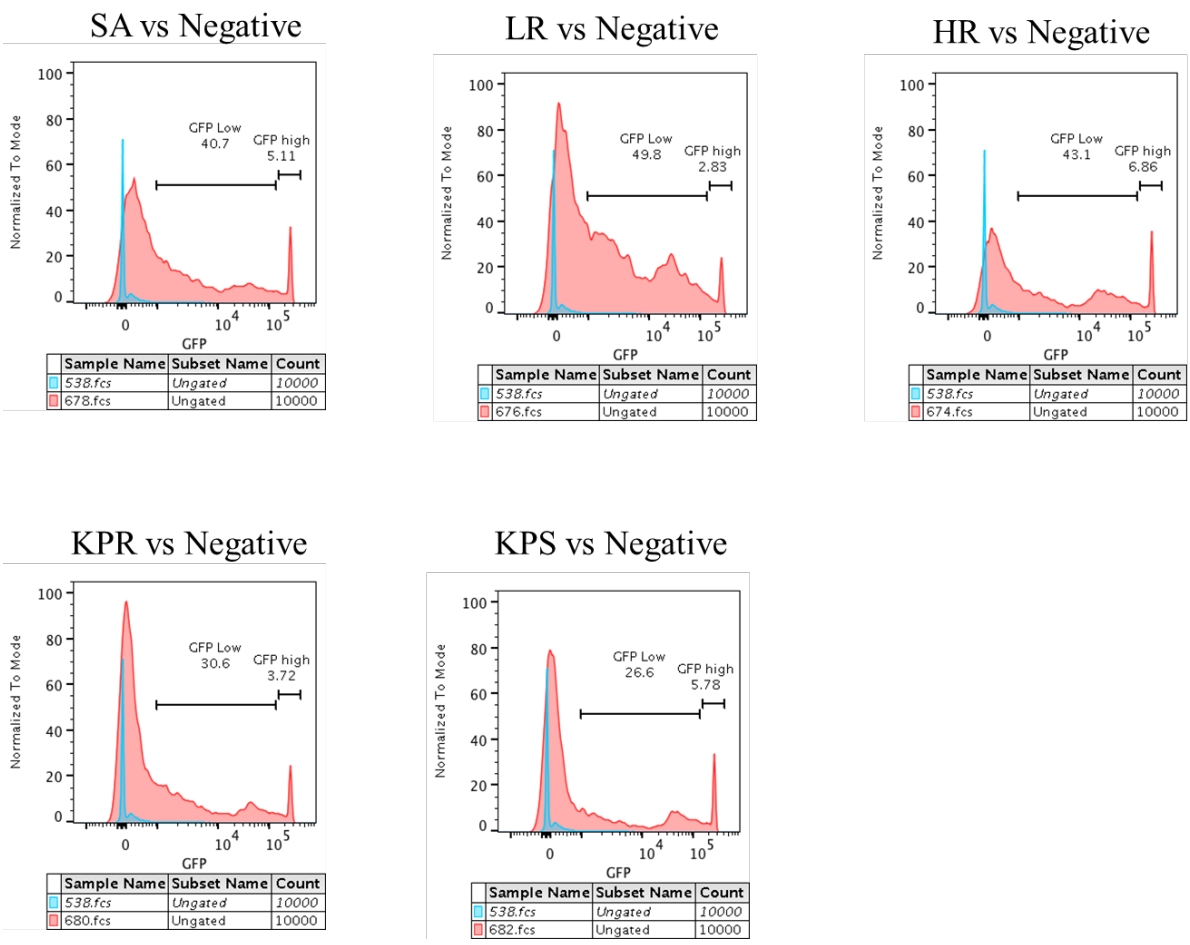

Figure 9-2-B Representative flow cytometry images color coded and compared to negative control

Flow cytometry images showing fluorescence intensity under each condition (pink) in comparison to the negative control (blue)
KPS: *K. pneumoniae* sensitive; KPR: *K. pneumoniae* resistant; MRSA LR: methicillin resistant *S. aureus* Low Resistance; MRSA HR: Methicillin Resistant *S. aureus* High Resistance.

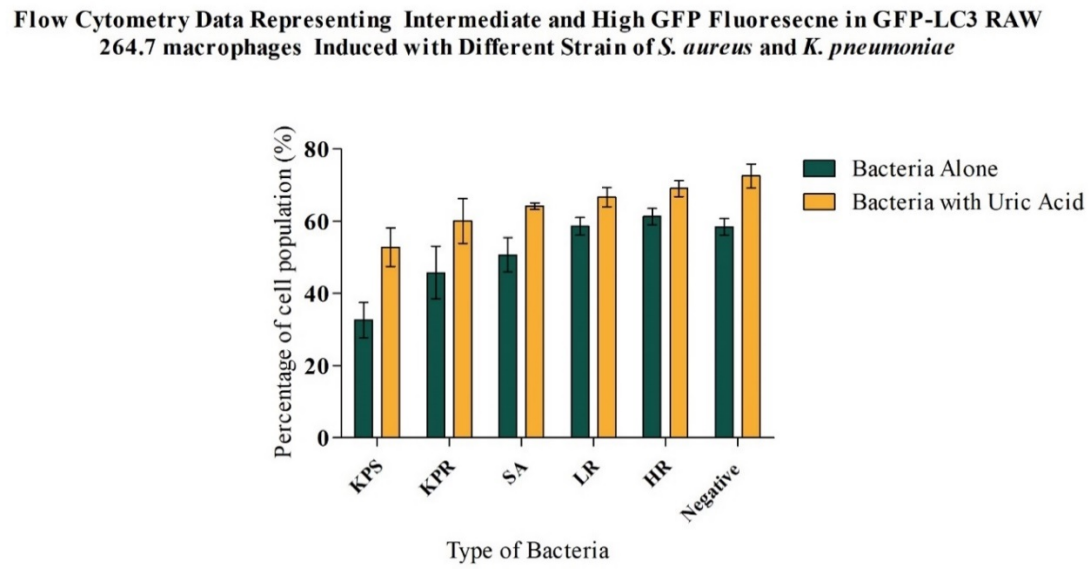

Figure 9-3 Flow cytometry GFP fluorescence data with GFP-LC3 RAW 264.7 Cell Line.

Data obtained using flow cytometry was used to create this graph. Percentage of cells with intermediate to high GFP fluorescence were calculated in each population.
KPS: *K. pneumoniae* sensitive; KPR: *K. pneumoniae* resistant; SA: *S. aureus*; MRSA LR: methicillin resistant *S. aureus* Low Resistance; MRSA HR: Methicillin Resistant *S. aureus* High Resistance.

10. References

1. Ohsumi Y. Historical landmarks of autophagy research. Cell Res. 2014;24(1):9-23.
2. Luciani A, Villella VR, Esposito S, Brunetti-Pierri N, Medina D, Settembre C, et al. Defective CFTR induces aggresome formation and lung inflammation in cystic fibrosis through ROS-mediated autophagy inhibition. Nature cell biology. 2010;12(9):863.
3. Lee S-J, Smith A, Guo L, Alastalo T-P, Li M, Sawada H, et al. Autophagic protein LC3B confers resistance against hypoxia-induced pulmonary hypertension. American journal of respiratory and critical care medicine. 2011;183(5):649-58.
4. Iida T, Onodera K, Nakase H. Role of autophagy in the pathogenesis of inflammatory bowel disease. World journal of gastroenterology. 2017;23(11):1944.
5. Yuk J-M, Jo E-K. Crosstalk between autophagy and inflammasomes. Molecules and cells. 2013;36(5):393-9.
6. Lopez-Castejon G, Brough D. Understanding the mechanism of IL-1β secretion. Cytokine & growth factor reviews. 2011;22(4):189-95.
7. Harris J, Hartman M, Roche C, Zeng SG, O'Shea A, Sharp FA, et al. Autophagy controls IL-1β secretion by targeting pro-IL-1β for degradation. Journal of Biological Chemistry. 2011;286(11):9587-97.
8. Park H-J, Pyo S. LPS-induced autophagy is mediated by nitric oxide in macrophages (P1285). Am Assoc Immnol; 2013.
9. Sarkar S, Korolchuk VI, Renna M, Imarisio S, Fleming A, Williams A, et al. Complex inhibitory effects of nitric oxide on autophagy. Molecular cell. 2011;43(1):19-32.
10. Huang J, Brumell JH. Bacteria–autophagy interplay: a battle for survival. Nature Reviews Microbiology. 2014;12(2):101.
11. De Duve C, Pressman B, Gianetto R, Wattiaux R, Appelmans F. Tissue fractionation studies. 6. Intracellular distribution patterns of enzymes in rat-liver tissue. Biochemical Journal. 1955;60(4):604.
12. De Duve C. The lysosome. Scientific American. 1963;208(5):64-73.
13. Arstila AU, Trump BF. Studies on cellular autophagocytosis. The formation of autophagic vacuoles in the liver after glucagon administration. The American journal of pathology. 1968;53(5):687.
14. Klionsky DJ. The molecular machinery of autophagy: unanswered questions. J Cell Sci. 2005;118(Pt 1):7-18.
15. Li WW, Li J, Bao JK. Microautophagy: lesser-known self-eating. Cell Mol Life Sci. 2012;69(7):1125-36.
16. Massey A, Kiffin R, Cuervo AM. Pathophysiology of chaperone-mediated autophagy. Int J Biochem Cell Biol. 2004;36(12):2420-34.
17. Reggiori F, Komatsu M, Finley K, Simonsen A. Autophagy: more than a nonselective pathway. International journal of cell biology. 2012;2012.
18. Klionsky DJ, Cuervo AM, Dunn J, William A, Levine B, van der Klei IJ, Seglen PO. How shall I eat thee? : Taylor & Francis; 2007.
19. Boya P, Reggiori F, Codogno P. Emerging regulation and functions of autophagy. Nat Cell Biol. 2013;15(7):713-20.
20. Schworer CM, Cox JR, Mortimore GE. Alteration of lysosomal density by sequestered glycogen during deprivation-induced autophagy in rat liver. Biochemical and biophysical research communications. 1979;87(1):163-70.

21. Komatsu M, Waguri S, Ueno T, Iwata J, Murata S, Tanida I, et al. Impairment of starvation-induced and constitutive autophagy in Atg7-deficient mice. J Cell Biol. 2005;169(3):425-34.
22. Nishino I. Autophagic vacuolar myopathies. Current neurology and neuroscience reports. 2003;3(1):64-9.
23. Komatsu M, Waguri S, Chiba T, Murata S, Iwata J-i, Tanida I, et al. Loss of autophagy in the central nervous system causes neurodegeneration in mice. Nature. 2006;441(7095):880-4.
24. Vidal R, Caballero B, Couve A, Hetz C. Converging pathways in the occurrence of endoplasmic reticulum (ER) stress in Huntington's disease. Current molecular medicine. 2011;11(1):1-12.
25. Galluzzi L, Pietrocola F, Bravo-San Pedro JM, Amaravadi RK, Baehrecke EH, Cecconi F, et al. Autophagy in malignant transformation and cancer progression. The EMBO journal. 2015;34(7):856-80.
26. White E, Mehnert JM, Chan CS. Autophagy, Metabolism, and Cancer. Clin Cancer Res. 2015;21(22):5037-46.
27. Schmid D, Pypaert M, Münz C. Antigen-loading compartments for major histocompatibility complex class II molecules continuously receive input from autophagosomes. Immunity. 2007;26(1):79-92.
28. Maejima I, Takahashi A, Omori H, Kimura T, Takabatake Y, Saitoh T, et al. Autophagy sequesters damaged lysosomes to control lysosomal biogenesis and kidney injury. The EMBO journal. 2013;32(17):2336-47.
29. Thurston TL, Wandel MP, von Muhlinen N, Foeglein Á, Randow F. Galectin 8 targets damaged vesicles for autophagy to defend cells against bacterial invasion. Nature. 2012;482(7385):414-8.
30. Zhao Z, Fux B, Goodwin M, Dunay IR, Strong D, Miller BC, et al. Autophagosome-independent essential function for the autophagy protein Atg5 in cellular immunity to intracellular pathogens. Cell host & microbe. 2008;4(5):458-69.
31. Huang J, Brumell JH. Bacteria-autophagy interplay: a battle for survival. Nature Reviews Microbiology. 2014;12(2):101-14.
32. Axe EL, Walker SA, Manifava M, Chandra P, Roderick HL, Habermann A, et al. Autophagosome formation from membrane compartments enriched in phosphatidylinositol 3-phosphate and dynamically connected to the endoplasmic reticulum. J Cell Biol. 2008;182(4):685-701.
33. Ganley IG, Lam dH, Wang J, Ding X, Chen S, Jiang X. ULK1· ATG13· FIP200 complex mediates mTOR signaling and is essential for autophagy. Journal of Biological Chemistry. 2009;284(18):12297-305.
34. Mercer CA, Kaliappan A, Dennis PB. A novel, human Atg13 binding protein, Atg101, interacts with ULK1 and is essential for macroautophagy. Autophagy. 2009;5(5):649-62.
35. Itakura E, Mizushima N. Atg14 and UVRAG: mutually exclusive subunits of mammalian Beclin 1-PI3K complexes. Autophagy. 2009;5(4):534-6.
36. Cao Y, Wang Y, Saab WFA, Yang F, Pessin JE, Backer JM. NRBF2 regulates macroautophagy as a component of Vps34 Complex I. Biochemical Journal. 2014;461(2):315-22.
37. Matsunaga K, Morita E, Saitoh T, Akira S, Ktistakis NT, Izumi T, et al. Autophagy requires endoplasmic reticulum targeting of the PI3-kinase complex via Atg14L. The Journal of cell biology. 2010;190(4):511-21.

38. Zhong Y, Wang QJ, Li X, Yan Y, Backer JM, Chait BT, et al. Distinct regulation of autophagic activity by Atg14L and Rubicon associated with Beclin 1–phosphatidylinositol-3-kinase complex. Nature cell biology. 2009;11(4):468-76.
39. Taguchi-Atarashi N, Hamasaki M, Matsunaga K, Omori H, Ktistakis NT, Yoshimori T, et al. Modulation of local PtdIns3P levels by the PI phosphatase MTMR3 regulates constitutive autophagy. Traffic. 2010;11(4):468-78.
40. Russell RC, Tian Y, Yuan H, Park HW, Chang Y-Y, Kim J, et al. ULK1 induces autophagy by phosphorylating Beclin-1 and activating VPS34 lipid kinase. Nature cell biology. 2013;15(7):741-50.
41. Polson HE, de Lartigue J, Rigden DJ, Reedijk M, Urbé S, Clague MJ, et al. Mammalian Atg18 (WIPI2) localizes to omegasome-anchored phagophores and positively regulates LC3 lipidation. Autophagy. 2010;6(4):506-22.
42. Orsi A, Razi M, Dooley H, Robinson D, Weston A, Collinson L, et al. Dynamic and transient interactions of Atg9 with autophagosomes, but not membrane integration, are required for autophagy. Molecular biology of the cell. 2012;23(10):1860-73.
43. Young AR, Chan EY, Hu XW, Köchl R, Crawshaw SG, High S, et al. Starvation and ULK1-dependent cycling of mammalian Atg9 between the TGN and endosomes. Journal of cell science. 2006;119(18):3888-900.
44. Ohsumi Y. Molecular dissection of autophagy: two ubiquitin-like systems. Nat Rev Mol Cell Biol. 2001;2(3):211-6.
45. Mizushima N, Kuma A, Kobayashi Y, Yamamoto A, Matsubae M, Takao T, et al. Mouse Apg16L, a novel WD-repeat protein, targets to the autophagic isolation membrane with the Apg12-Apg5 conjugate. Journal of cell science. 2003;116(9):1679-88.
46. Kuma A, Mizushima N, Ishihara N, Ohsumi Y. Formation of the~ 350-kDa Apg12-Apg5· Apg16 multimeric complex, mediated by Apg16 oligomerization, is essential for autophagy in yeast. Journal of Biological Chemistry. 2002;277(21):18619-25.
47. Hanada T, Noda NN, Satomi Y, Ichimura Y, Fujioka Y, Takao T, et al. The Atg12-Atg5 conjugate has a novel E3-like activity for protein lipidation in autophagy. Journal of Biological Chemistry. 2007;282(52):37298-302.
48. McEwan DG, Popovic D, Gubas A, Terawaki S, Suzuki H, Stadel D, et al. PLEKHM1 regulates autophagosome-lysosome fusion through HOPS complex and LC3/GABARAP proteins. Molecular cell. 2015;57(1):39-54.
49. Gutierrez MG, Munafó DB, Berón W, Colombo MI. Rab7 is required for the normal progression of the autophagic pathway in mammalian cells. Journal of cell science. 2004;117(13):2687-97.
50. Moreau K, Ravikumar B, Renna M, Puri C, Rubinsztein DC. Autophagosome precursor maturation requires homotypic fusion. Cell. 2011;146(2):303-17.
51. Hegedűs K, Takáts S, Kovács AL, Juhász G. Evolutionarily conserved role and physiological relevance of a STX17/Syx17 (syntaxin 17)-containing SNARE complex in autophagosome fusion with endosomes and lysosomes. Autophagy. 2013;9(10):1642-6.
52. Tsuboyama K, Koyama-Honda I, Sakamaki Y, Koike M, Morishita H, Mizushima N. The ATG conjugation systems are important for degradation of the inner autophagosomal membrane. Science. 2016;354(6315):1036-41.
53. Neufeld TP. TOR-dependent control of autophagy: biting the hand that feeds. Current opinion in cell biology. 2010;22(2):157-68.

54. Xu Y, Jagannath C, Liu X-D, Sharafkhaneh A, Kolodziejska KE, Eissa NT. Toll-like receptor 4 is a sensor for autophagy associated with innate immunity. Immunity. 2007;27(1):135-44.
55. Lee HK, Lund JM, Ramanathan B, Mizushima N, Iwasaki A. Autophagy-dependent viral recognition by plasmacytoid dendritic cells. Science. 2007;315(5817):1398-401.
56. Travassos LH, Carneiro LA, Ramjeet M, Hussey S, Kim Y-G, Magalhães JG, et al. Nod1 and Nod2 direct autophagy by recruiting ATG16L1 to the plasma membrane at the site of bacterial entry. Nature immunology. 2010;11(1):55-62.
57. Lei Y, Wen H, Yu Y, Taxman DJ, Zhang L, Widman DG, et al. The mitochondrial proteins NLRX1 and TUFM form a complex that regulates type I interferon and autophagy. Immunity. 2012;36(6):933-46.
58. Gajewska M, Gajkowska B, Motyl T. Apoptosis and autophagy induced by TGF-ß1 in bovine mammary epithelial BME-UV1 cells. J Physiol Pharmacol. 2005;56(Suppl 3):143-57.
59. Xu Y, Yang S, Huang J, Ruan S, Zheng Z, Lin J. Tgf-β1 induces autophagy and promotes apoptosis in renal tubular epithelial cells. International journal of molecular medicine. 2012;29(5):781-90.
60. Guido C, Whitaker-Menezes D, Capparelli C, Balliet R, Lin Z, Pestell RG, et al. Metabolic reprogramming of cancer-associated fibroblasts by TGF-β drives tumor growth: connecting TGF-β signaling with "Warburg-like" cancer metabolism and L-lactate production. Cell cycle. 2012;11(16):3019-35.
61. Ghavami S, Cunnington RH, Gupta S, Yeganeh B, Filomeno KL, Freed DH, et al. Autophagy is a regulator of TGF-beta1-induced fibrogenesis in primary human atrial myofibroblasts. Cell Death Dis. 2015;6:e1696.
62. Patel AS, Lin L, Geyer A, Haspel JA, An CH, Cao J, et al. Autophagy in idiopathic pulmonary fibrosis. PloS one. 2012;7(7):e41394.
63. Gutierrez MG, Master SS, Singh SB, Taylor GA, Colombo MI, Deretic V. Autophagy is a defense mechanism inhibiting BCG and Mycobacterium tuberculosis survival in infected macrophages. Cell. 2004;119(6):753-66.
64. Oh S-Y, Choi S-J, Kim KH, Cho E, Kim J-H, Roh C-R. Autophagy-related proteins, LC3 and Beclin-1, in placentas from pregnancies complicated by preeclampsia. Reproductive sciences. 2008;15(9):912-20.
65. Lotze MT, Buchser W, Liang X. Blocking the interleukin 2 (IL2)-induced systemic autophagic syndrome promotes profound antitumor effects and limits toxicity. Autophagy. 2012;8(8):1264-6.
66. Shi CS, Kehrl JH. TRAF6 and A20 regulate lysine 63-linked ubiquitination of Beclin-1 to control TLR4-induced autophagy. Sci Signal. 2010;3(123):ra42.
67. Peral de Castro C, Jones SA, Ni Cheallaigh C, Hearnden CA, Williams L, Winter J, et al. Autophagy regulates IL-23 secretion and innate T cell responses through effects on IL-1 secretion. J Immunol. 2012;189(8):4144-53.
68. Tang D, Kang R, Livesey KM, Cheh CW, Farkas A, Loughran P, et al. Endogenous HMGB1 regulates autophagy. J Cell Biol. 2010;190(5):881-92.
69. Muñoz-Gámez JA, Rodríguez-Vargas JM, Quiles-Pérez R, Aguilar-Quesada R, Martín-Oliva D, de Murcia G, et al. PARP-1 is involved in autophagy induced by DNA damage. Autophagy. 2009;5(1):61-74.

70. Foell D, Wittkowski H, Vogl T, Roth J. S100 proteins expressed in phagocytes: a novel group of damage-associated molecular pattern molecules. Journal of leukocyte biology. 2007;81(1):28-37.
71. Ghavami S, Eshragi M, Ande SR, Chazin WJ, Klonisch T, Halayko AJ, et al. S100A8/A9 induces autophagy and apoptosis via ROS-mediated cross-talk between mitochondria and lysosomes that involves BNIP3. Cell research. 2010;20(3):314-31.
72. Martinon F, Burns K, Tschopp J. The inflammasome: a molecular platform triggering activation of inflammatory caspases and processing of proIL-β. Molecular cell. 2002;10(2):417-26.
73. Davis BK, Wen H, Ting JP-Y. The inflammasome NLRs in immunity, inflammation, and associated diseases. Annual review of immunology. 2011;29:707-35.
74. Hoffman HM, Mueller JL, Broide DH, Wanderer AA, Kolodner RD. Mutation of a new gene encoding a putative pyrin-like protein causes familial cold autoinflammatory syndrome and Muckle–Wells syndrome. Nature genetics. 2001;29(3):301-5.
75. Vanaja SK, Rathinam VA, Fitzgerald KA. Mechanisms of inflammasome activation: recent advances and novel insights. Trends in cell biology. 2015;25(5):308-15.
76. Lamkanfi M. Emerging inflammasome effector mechanisms. Nature Reviews Immunology. 2011;11(3):213-20.
77. Tschopp J, Schroder K. NLRP3 inflammasome activation: The convergence of multiple signalling pathways on ROS production? Nature Reviews Immunology. 2010;10(3):210-5.
78. Chavarría-Smith J, Vance RE. The NLRP1 inflammasomes. Immunological reviews. 2015;265(1):22-34.
79. Zhao Y, Shao F. The NAIP–NLRC4 inflammasome in innate immune detection of bacterial flagellin and type III secretion apparatus. Immunological reviews. 2015;265(1):85-102.
80. Man SM, Karki R, Kanneganti TD. AIM2 inflammasome in infection, cancer, and autoimmunity: Role in DNA sensing, inflammation, and innate immunity. European journal of immunology. 2016;46(2):269-80.
81. Xu H, Yang J, Gao W, Li L, Li P, Zhang L, et al. Innate immune sensing of bacterial modifications of Rho GTPases by the Pyrin inflammasome. Nature. 2014;513(7517):237-41.
82. Milhavet F, Cuisset L, Hoffman HM, Slim R, El-Shanti H, Aksentijevich I, et al. The infevers autoinflammatory mutation online registry: update with new genes and functions. Human mutation. 2008;29(6):803-8.
83. Foster MW, Hess DT, Stamler JS. Protein S-nitrosylation in health and disease: a current perspective. Trends in molecular medicine. 2009;15(9):391-404.
84. Murad F. Nitric oxide and cyclic GMP in cell signaling and drug development. New England Journal of Medicine. 2006;355(19):2003-11.
85. Thomassen MJ, Buhrow LT, Connors MJ, Takao Kaneko F, Erzurum SC, Kavuru MS. Nitric oxide inhibits inflammatory cytokine production by human alveolar macrophages. American Journal of Respiratory Cell and Molecular Biology. 1997;17(3):279-83.
86. Kim Y-M, Talanian RV, Li J, Billiar TR. Nitric oxide prevents IL-1β and IFN-γ-inducing factor (IL-18) release from macrophages by inhibiting caspase-1 (IL-1β-converting enzyme). The Journal of Immunology. 1998;161(8):4122-8.
87. Chang K, Lee S-J, Cheong I, Billiar TR, Chung H-T, Han J-A, et al. Nitric oxide suppresses inducible nitric oxide synthase expression by inhibiting post-translational modification of IκB. Experimental & molecular medicine. 2004;36(4):311.

88. Lee J, Giordano S, Zhang J. Autophagy, mitochondria and oxidative stress: cross-talk and redox signalling. Biochemical Journal. 2012;441(2):523-40.
89. Barsoum MJ, Yuan H, Gerencser AA, Liot G, Kushnareva Y, Gräber S, et al. Nitric oxide-induced mitochondrial fission is regulated by dynamin-related GTPases in neurons. The EMBO journal. 2006;25(16):3900-11.
90. Fan S, Li L, Chen S, Yu Y, Qi M, Tashiro S-I, et al. Silibinin induced-autophagic and apoptotic death is associated with an increase in reactive oxygen and nitrogen species in HeLa cells. Free radical research. 2011;45(11-12):1307-24.
91. Pestana CR, Oishi JC, Salistre-Araújo HS, Rodrigues GJ. Inhibition of autophagy by chloroquine stimulates nitric oxide production and protects endothelial function during serum deprivation. Cellular Physiology and Biochemistry. 2015;37(3):1168-77.
92. Martinon F. Update on biology: uric acid and the activation of immune and inflammatory cells. Current rheumatology reports. 2010;12(2):135-41.
93. Johnson RJ, Lanaspa MA, Gaucher EA. Uric acid: a danger signal from the RNA world that may have a role in the epidemic of obesity, metabolic syndrome, and cardiorenal disease: evolutionary considerations. Semin Nephrol. 2011;31(5):394-9.
94. Cicerchi C, Li N, Kratzer J, Garcia G, Roncal-Jimenez CA, Tanabe K, et al. Uric acid-dependent inhibition of AMP kinase induces hepatic glucose production in diabetes and starvation: evolutionary implications of the uricase loss in hominids. FASEB J. 2014;28(8):3339-50.
95. Ames BN, Cathcart R, Schwiers E, Hochstein P. Uric acid provides an antioxidant defense in humans against oxidant-and radical-caused aging and cancer: a hypothesis. Proceedings of the National Academy of Sciences. 1981;78(11):6858-62.
96. Sautin YY, Nakagawa T, Zharikov S, Johnson RJ. Adverse effects of the classic antioxidant uric acid in adipocytes: NADPH oxidase-mediated oxidative/nitrosative stress. American Journal of Physiology-Cell Physiology. 2007;293(2):C584-C96.
97. Heazlewood CK, Cook MC, Eri R, Price GR, Tauro SB, Taupin D, et al. Aberrant mucin assembly in mice causes endoplasmic reticulum stress and spontaneous inflammation resembling ulcerative colitis. PLoS medicine. 2008;5(3):e54.
98. van den Berghe G, Vincent M-F, Marie S. Disorders of purine and pyrimidine metabolism. Inborn Metabolic Diseases: Springer; 2012. p. 499-518.
99. Loeb JN. The influence of temperature on the solubility of monosodium urate. Arthritis & Rheumatology. 1972;15(2):189-92.
100. Wilcox WR, Khalaf A. Nucleation of monosodium urate crystals. Annals of the rheumatic diseases. 1975;34(4):332-9.
101. DeFranco AL. Dangerous crystals. Immunity. 2008;29(5):670-1.
102. Landis RC, Haskard DO. Pathogenesis of crystal-induced inflammation. Current rheumatology reports. 2001;3(1):36-41.
103. Nagase M, Baker D, Schumacher Jr HR. Immunoglobulin G coating on crystals and ceramics enhances polymorphonuclear cell superoxide production: correlation with immunoglobulin G adsorbed. The Journal of rheumatology. 1989;16(7):971-6.
104. Barabé F, Gilbert C, Liao N, Bourgoin SG, Naccache PH. Crystal-induced neutrophil activation VI. Involvement of FcγRIIIB (CD16) and CD11b in response to inflammatory microcrystals. The FASEB journal. 1998;12(2):209-20.

105. Gasse P, Riteau N, Charron S, Girre S, Fick L, Pétrilli V, et al. Uric acid is a danger signal activating NALP3 inflammasome in lung injury inflammation and fibrosis. American journal of respiratory and critical care medicine. 2009;179(10):903-13.
106. Martinon F, Pétrilli V, Mayor A, Tardivel A, Tschopp J. Gout-associated uric acid crystals activate the NALP3 inflammasome. Nature. 2006;440(7081):237-41.
107. Petrilli V, Papin S, Dostert C, Mayor A, Martinon F, Tschopp J. Activation of the NALP3 inflammasome is triggered by low intracellular potassium concentration. Cell Death & Differentiation. 2007;14(9):1583-9.
108. Cannon GJ, Swanson JA. The macrophage capacity for phagocytosis. Journal of cell science. 1992;101(4):907-13.
109. Hoffstein S, Weissmann G. Mechanisms of lysosomal enzyme release from leukocytes. Arthritis & Rheumatology. 1975;18(2):153-65.
110. Hornung V, Bauernfeind F, Halle A, Samstad EO, Kono H, Rock KL, et al. Silica crystals and aluminum salts activate the NALP3 inflammasome through phagosomal destabilization. Nature immunology. 2008;9(8):847-56.
111. Braga TT, Forni MF, Correa-Costa M, Ramos RN, Barbuto JA, Branco P, et al. Soluble uric acid activates the NLRP3 inflammasome. Scientific reports. 2017;7.
112. Hui M, Carr A, Cameron S, Davenport G, Doherty M, Forrester H, et al. The British Society for Rheumatology guideline for the management of gout. Rheumatology. 2017;56(7):1056-9.
113. Zhu Y, Pandya BJ, Choi HK. Prevalence of gout and hyperuricemia in the US general population: the National Health and Nutrition Examination Survey 2007–2008. Arthritis & Rheumatology. 2011;63(10):3136-41.
114. Reginato AM, Mount DB, Yang I, Choi HK. The genetics of hyperuricaemia and gout. Nat Rev Rheumatol. 2012;8(10):610-21.
115. Mandell BF. Clinical manifestations of hyperuricemia and gout. Cleveland Clinic journal of medicine. 2008;75:S5-8.
116. Matias ML, Romao M, Weel IC, Ribeiro VR, Nunes PR, Borges VT, et al. Endogenous and uric acid-induced activation of NLRP3 inflammasome in pregnant women with preeclampsia. PloS one. 2015;10(6):e0129095.
117. Momoki K, Kataoka H, Moriyama T, Mochizuki T, Nitta K. Hyperuricemia as a Predictive Marker for Progression of Nephrosclerosis: Clinical Assessment of Prognostic Factors in Biopsy-Proven Arterial/Arteriolar Nephrosclerosis. Journal of atherosclerosis and thrombosis. 2017;24(6):630-42.
118. Yue C-F, Feng P-N, Yao Z-R, Yu X-G, Lin W-b, Qian Y-M, et al. High serum uric acid concentration predicts poor survival in patients with breast cancer. Clinica Chimica Acta. 2017;473:160-5.
119. Billiet L, Doaty S, Katz JD, Velasquez MT. Review of hyperuricemia as new marker for metabolic syndrome. ISRN rheumatology. 2014;2014.
120. Saitoh T, Fujita N, Jang MH, Uematsu S, Yang B-G, Satoh T, et al. Loss of the autophagy protein Atg16L1 enhances endotoxin-induced IL-1β production. Nature. 2008;456(7219):264-8.
121. Nakahira K, Haspel JA, Rathinam VA, Lee S-J, Dolinay T, Lam HC, et al. Autophagy proteins regulate innate immune responses by inhibiting the release of mitochondrial DNA mediated by the NALP3 inflammasome. Nature immunology. 2011;12(3):222-30.

122. Zhou R, Yazdi AS, Menu P, Tschopp J. A role for mitochondria in NLRP3 inflammasome activation. Nature. 2011;469(7329):221-5.
123. Shi C-S, Shenderov K, Huang N-N, Kabat J, Abu-Asab M, Fitzgerald KA, et al. Activation of autophagy by inflammatory signals limits IL-1 [beta] production by targeting ubiquitinated inflammasomes for destruction. Nature immunology. 2012;13(3):255-63.
124. Kraft C, Peter M, Hofmann K. Selective autophagy: ubiquitin-mediated recognition and beyond. Nature cell biology. 2010;12(9):836-41.
125. Knodler LA, Celli J. Eating the strangers within: host control of intracellular bacteria via xenophagy. Cellular microbiology. 2011;13(9):1319-27.
126. Nakagawa I, Amano A, Mizushima N, Yamamoto A, Yamaguchi H, Kamimoto T, et al. Autophagy defends cells against invading group A Streptococcus. Science. 2004;306(5698):1037-40.
127. Yamaguchi H, Nakagawa I, Yamamoto A, Amano A, Noda T, Yoshimori T. An initial step of GAS-containing autophagosome-like vacuoles formation requires Rab7. PLoS pathogens. 2009;5(11):e1000670.
128. Tattoli I, Sorbara MT, Vuckovic D, Ling A, Soares F, Carneiro LA, et al. Amino acid starvation induced by invasive bacterial pathogens triggers an innate host defense program. Cell host & microbe. 2012;11(6):563-75.
129. Kim KH, An DR, Song J, Yoon JY, Kim HS, Yoon HJ, et al. Mycobacterium tuberculosis Eis protein initiates suppression of host immune responses by acetylation of DUSP16/MKP-7. Proceedings of the National Academy of Sciences. 2012;109(20):7729-34.
130. Shin D-M, Jeon B-Y, Lee H-M, Jin HS, Yuk J-M, Song C-H, et al. Mycobacterium tuberculosis eis regulates autophagy, inflammation, and cell death through redox-dependent signaling. PLoS pathogens. 2010;6(12):e1001230.
131. Dong N, Zhu Y, Lu Q, Hu L, Zheng Y, Shao F. Structurally distinct bacterial TBC-like GAPs link Arf GTPase to Rab1 inactivation to counteract host defenses. Cell. 2012;150(5):1029-41.
132. Huang J, Birmingham CL, Shahnazari S, Shiu J, Zheng YT, Smith AC, et al. Antibacterial autophagy occurs at PI (3) P-enriched domains of the endoplasmic reticulum and requires Rab1 GTPase. Autophagy. 2011;7(1):17-26.
133. Choy A, Dancourt J, Mugo B, O'Connor TJ, Isberg RR, Melia TJ, et al. The Legionella effector RavZ inhibits host autophagy through irreversible Atg8 deconjugation. Science. 2012;338(6110):1072-6.
134. Ogawa M, Yoshimori T, Suzuki T, Sagara H, Mizushima N, Sasakawa C. Escape of intracellular Shigella from autophagy. Science. 2005;307(5710):727-31.
135. Mostowy S, Bonazzi M, Hamon MA, Tham TN, Mallet A, Lelek M, et al. Entrapment of intracytosolic bacteria by septin cage-like structures. Cell host & microbe. 2010;8(5):433-44.
136. Lerena MC, Colombo MI. Mycobacterium marinum induces a marked LC3 recruitment to its containing phagosome that depends on a functional ESX-1 secretion system. Cellular microbiology. 2011;13(6):814-35.
137. Lapaquette P, Bringer MA, Darfeuille-Michaud A. Defects in autophagy favour adherent-invasive Escherichia coli persistence within macrophages leading to increased pro-inflammatory response. Cellular microbiology. 2012;14(6):791-807.
138. Schnaith A, Kashkar H, Leggio SA, Addicks K, Krönke M, Krut O. Staphylococcus aureus subvert autophagy for induction of caspase-independent host cell death. Journal of Biological Chemistry. 2007;282(4):2695-706.

139. Gutierrez MG, Vázquez CL, Munafó DB, Zoppino F, Berón W, Rabinovitch M, et al. Autophagy induction favours the generation and maturation of the Coxiella-replicative vacuoles. Cellular microbiology. 2005;7(7):981-93.
140. Vazquez C, Colombo M. Coxiella burnetii modulates Beclin 1 and Bcl-2, preventing host cell apoptosis to generate a persistent bacterial infection. Cell Death & Differentiation. 2010;17(3):421-38.
141. Gong L, Cullinane M, Treerat P, Ramm G, Prescott M, Adler B, et al. The Burkholderia pseudomallei type III secretion system and BopA are required for evasion of LC3-associated phagocytosis. PloS one. 2011;6(3):e17852.
142. Netea-Maier RT, Plantinga TS, van de Veerdonk FL, Smit JW, Netea MG. Modulation of inflammation by autophagy: consequences for human disease. Autophagy. 2016;12(2):245-60.
143. Soltani Z, Rasheed K, Kapusta DR, Reisin E. Potential role of uric acid in metabolic syndrome, hypertension, kidney injury, and cardiovascular diseases: is it time for reappraisal? Current hypertension reports. 2013;15(3):175-81.
144. Shi C-S, Shenderov K, Huang N-N, Kabat J, Abu-Asab M, Fitzgerald KA, et al. Activation of autophagy by inflammatory signals limits IL-1β production by targeting ubiquitinated inflammasomes for destruction. Nature immunology. 2012;13(3):255.
145. Dinarello CA. The history of fever, leukocytic pyrogen and interleukin-1. Taylor & Francis; 2015.
146. Gabay C, Lamacchia C, Palmer G. IL-1 pathways in inflammation and human diseases. Nature Reviews Rheumatology. 2010;6(4):232.
147. Sollberger G, Strittmatter GE, Garstkiewicz M, Sand J, Beer H-D. Caspase-1: the inflammasome and beyond. Innate immunity. 2014;20(2):115-25.
148. Martinon F, Pétrilli V, Mayor A, Tardivel A, Tschopp J. Gout-associated uric acid crystals activate the NALP3 inflammasome. Nature. 2006;440(7081):237.
149. Braga TT, Forni MF, Correa-Costa M, Ramos RN, Barbuto JA, Branco P, et al. Soluble uric acid activates the NLRP3 inflammasome. Scientific reports. 2017;7:39884.
150. Mao K, Chen S, Chen M, Ma Y, Wang Y, Huang B, et al. Nitric oxide suppresses NLRP3 inflammasome activation and protects against LPS-induced septic shock. Cell research. 2013;23(2):201.
151. Miyasaka N, Hirata Y. Nitric oxide and inflammatory arthritides. Life sciences. 1997;61(21):2073-81.
152. Sun J, Zhang X, Broderick M, Fein H. Measurement of nitric oxide production in biological systems by using Griess reaction assay. Sensors. 2003;3(8):276-84.
153. Ohsumi Y. Historical landmarks of autophagy research. Cell research. 2014;24(1):9.
154. Takahama M, Akira S, Saitoh T. Autophagy limits activation of the inflammasomes. Immunological reviews. 2018;281(1):62-73.
155. Mestre MB, Colombo MI. Staphylococcus aureus promotes autophagy by decreasing intracellular cAMP levels. Autophagy. 2012;8(12):1865-7.
156. Neumann Y, Bruns SA, Rohde M, Prajsnar TK, Foster SJ, Schmitz I. Intracellular Staphylococcus aureus eludes selective autophagy by activating a host cell kinase. Autophagy. 2016;12(11):2069-84.
157. Fang L, Wu H-M, Ding P-S, Liu R-Y. TLR2 mediates phagocytosis and autophagy through JNK signaling pathway in Staphylococcus aureus-stimulated RAW264. 7 cells. Cellular signalling. 2014;26(4):806-14.

158. Maurer K, Reyes-Robles T, Alonzo III F, Durbin J, Torres VJ, Cadwell K. Autophagy mediates tolerance to Staphylococcus aureus alpha-toxin. Cell host & microbe. 2015;17(4):429-40.
159. Flannagan RS, Heit B, Heinrichs DE. Intracellular replication of Staphylococcus aureus in mature phagolysosomes in macrophages precedes host cell death, and bacterial escape and dissemination. Cellular microbiology. 2016;18(4):514-35.
160. Li X, He S, Zhou X, Ye Y, Tan S, Zhang S, et al. Lyn delivers bacteria to lysosomes for eradication through TLR2-initiated autophagy related phagocytosis. PLoS pathogens. 2016;12(1):e1005363.
161. Crişan TO, Cleophas MC, Novakovic B, Erler K, van de Veerdonk FL, Stunnenberg HG, et al. Uric acid priming in human monocytes is driven by the AKT–PRAS40 autophagy pathway. Proceedings of the National Academy of Sciences. 2017;114(21):5485-90.
162. Allaeys I, Marceau F, Poubelle PE. NLRP3 promotes autophagy of urate crystals phagocytized by human osteoblasts. Arthritis research & therapy. 2013;15(6):R176.
163. Hung Y-H, Chen LM-W, Yang J-Y, Yang WY. Spatiotemporally controlled induction of autophagy-mediated lysosome turnover. Nature communications. 2013;4:2111.
164. Sautin YY, Johnson RJ. Uric acid: the oxidant-antioxidant paradox. Nucleosides, Nucleotides, and Nucleic Acids. 2008;27(6-7):608-19.
165. Gurung P, Lukens JR, Kanneganti T-D. Mitochondria: diversity in the regulation of the NLRP3 inflammasome. Trends in molecular medicine. 2015;21(3):193-201.
166. McGilligan VE, Gregory-Ksander MS, Li D, Moore JE, Hodges RR, Gilmore MS, et al. Staphylococcus aureus activates the NLRP3 inflammasome in human and rat conjunctival goblet cells. PLoS One. 2013;8(9):e74010.
167. Mariathasan S, Weiss DS, Newton K, McBride J, O'rourke K, Roose-Girma M, et al. Cryopyrin activates the inflammasome in response to toxins and ATP. Nature. 2006;440(7081):228.
168. Kebaier C, Chamberland RR, Allen IC, Gao X, Broglie PM, Hall JD, et al. Staphylococcus aureus α-hemolysin mediates virulence in a murine model of severe pneumonia through activation of the NLRP3 inflammasome. Journal of Infectious Diseases. 2012;205(5):807-17.
169. Willingham SB, Allen IC, Bergstralh DT, Brickey WJ, Huang MT-H, Taxman DJ, et al. NLRP3 (NALP3, Cryopyrin) facilitates in vivo caspase-1 activation, necrosis, and HMGB1 release via inflammasome-dependent and-independent pathways. The Journal of Immunology. 2009;183(3):2008-15.
170. Hua K-F, Yang F-L, Chiu H-W, Chou J-C, Dong W-C, Lin C-N, et al. Capsular polysaccharide is involved in NLRP3 inflammasome activation by Klebsiella pneumoniae serotype K1. Infection and immunity. 2015;83(9):3396-409.
171. Günther J, Esch K, Poschadel N, Petzl W, Zerbe H, Mitterhuemer S, et al. Comparative kinetics of Escherichia coli-and Staphylococcus aureus-specific activation of key immune pathways in mammary epithelial cells demonstrates that S. aureus elicits a delayed response dominated by interleukin-6 (IL-6) but not by IL-1A or tumor necrosis factor alpha. Infection and immunity. 2011;79(2):695-707.
172. Poltorak A, He X, Smirnova I, Liu M-Y, Van Huffel C, Du X, et al. Defective LPS signaling in C3H/HeJ and C57BL/10ScCr mice: mutations in Tlr4 gene. Science. 1998;282(5396):2085-8.

173. Schwandner R, Dziarski R, Wesche H, Rothe M, Kirschning CJ. Peptidoglycan-and lipoteichoic acid-induced cell activation is mediated by toll-like receptor 2. Journal of Biological Chemistry. 1999;274(25):17406-9.
174. Shi Y, Evans JE, Rock KL. Molecular identification of a danger signal that alerts the immune system to dying cells. Nature. 2003;425(6957):516.
175. Piancone F, Saresella M, Marventano I, La Rosa F, Santangelo MA, Caputo D, et al. Monosodium Urate Crystals Activate the Inflammasome in Primary Progressive Multiple Sclerosis. Frontiers in Immunology. 2018;9:983.
176. MacMicking J, Xie Q-w, Nathan C. Nitric oxide and macrophage function. Annual review of immunology. 1997;15(1):323-50.
177. Bogdan C. Nitric oxide and the immune response. Nature immunology. 2001;2(10):907.
178. Hernandez-Cuellar E, Tsuchiya K, Hara H, Fang R, Sakai S, Kawamura I, et al. Cutting edge: nitric oxide inhibits the NLRP3 inflammasome. The Journal of Immunology. 2012;189(11):5113-7.
179. Sasaki S, Miura T, Nishikawa S, Yamada K, Hirasue M, Nakane A. Protective Role of Nitric Oxide inStaphylococcus aureus Infection in Mice. Infection and Immunity. 1998;66(3):1017-22.
180. Carey RM, Workman AD, Chen B, Adappa ND, Palmer JN, Kennedy DW, et al., editors. Staphylococcus aureus triggers nitric oxide production in human upper airway epithelium. International forum of allergy & rhinology; 2015: Wiley Online Library.
181. Kim NJ, Ahn KB, Jeon JH, Yun C-H, Finlay BB, Han SH. Lipoprotein in the cell wall of Staphylococcus aureus is a major inducer of nitric oxide production in murine macrophages. Molecular immunology. 2015;65(1):17-24.
182. Tsai WC, Strieter RM, Zisman DA, Wilkowski JM, Bucknell KA, Chen G-H, et al. Nitric oxide is required for effective innate immunity against Klebsiella pneumoniae. Infection and immunity. 1997;65(5):1870-5.
183. Xie Q, Kashiwabara Y, Nathan C. Role of transcription factor NF-kappa B/Rel in induction of nitric oxide synthase. Journal of Biological Chemistry. 1994;269(7):4705-8.
184. Kengatharan M, Kimpe SJ, Thiemermann C. Analysis of the signal transduction in the induction of nitric oxide synthase by lipoteichoic acid in macrophages. British journal of pharmacology. 1996;117(6):1163-70.
185. Yang K, Wu Y, Xie H, Li M, Ming S, Li L, et al. Macrophage-mediated inflammatory response decreases mycobacterial survival in mouse MSCs by augmenting NO production. Scientific reports. 2016;6:27326.
186. Gersch C, Palii SP, Kim KM, Angerhofer A, Johnson RJ, Henderson GN. Inactivation of nitric oxide by uric acid. Nucleosides, Nucleotides and Nucleic Acids. 2008;27(8):967-78.
187. Khosla UM, Zharikov S, Finch JL, Nakagawa T, Roncal C, Mu W, et al. Hyperuricemia induces endothelial dysfunction. Kidney international. 2005;67(5):1739-42.
188. Jaramillo M, Naccache PH, Olivier M. Monosodium urate crystals synergize with IFN-γ to generate macrophage nitric oxide: involvement of extracellular signal-regulated kinase 1/2 and NF-κB. The Journal of Immunology. 2004;172(9):5734-42.
189. Chen L, Hsieh M-S, Ho H-C, Liu Y-H, Chou D-T, Tsai S-H. Stimulation of inducible nitric oxide synthase by monosodium urate crystals in macrophages and expression of iNOS in gouty arthritis. Nitric Oxide. 2004;11(3):228-36.
190. Liu-Bryan R, Scott P, Sydlaske A, Rose DM, Terkeltaub R. Innate immunity conferred by toll-like receptors 2 and 4 and myeloid differentiation factor 88 expression is pivotal to

monosodium urate monohydrate crystal–induced inflammation. Arthritis & Rheumatology. 2005;52(9):2936-46.